Marine Environmental Research
September 2024, Volume 200, Pages 106653 (15p.)
https://doi.org/10.1016/j.marenvres.2024.106653 https://archimer.ifremer.fr/doc/00901/101337/

Archimer
https://archimer.ifremer.fr

Ecology of *Bathymodiolus puteoserpentis* mussels from the Snake Pit vent field (Mid-Atlantic Ridge)

Veuillot Alicia [1], Pradillon Florence [1], Michel Loïc [2], Cathalot Cécile [3], Cambon Marie-Anne [1], Sarrazin Jozée [1, *]

[1] Univ Brest, Ifremer, Unité BEEP, Plouzané, France
[2] Univ Liège, Unité FOCUS, Liège, Belgique
[3] Univ Brest, Ifremer, CNRS, Unité GEOCEAN, Plouzané, France

* Corresponding author : Jozée Sarrazin, email address : Jozee.Sarrazin@ifremer.fr

Abstract :

Along the northern Mid-Atlantic Ridge (nMAR), in habitats under moderate (<10°C) hydrothermal influence on the Snake Pit vent field (SP), large assemblages dominated by Bathymodiolin mussels remain poorly characterised, contrary to those in warmer habitats dominated by gastropods and alvinocaridid shrimps that were recently described. In this study, we assessed and compared the population structure, biomass, diversity and trophic interactions of two Bathymodiolus puteoserpentis assemblages and their associated fauna at SP. Three sampling units distanced by 30 cm were sampled in 2014 during the BICOSE cruise at the top of the Moose site (''Elan'' site), while few meters further down three others, distanced by ~1 m were obtained in 2018 during the BICOSE 2 cruise at the edifice's base. We observed a micro-scale heterogeneity between these six sampling units partially explained by temperature variations, proximity to hydrothermal fluids and position on the edifice. Meiofauna dominate or co-dominate most of the sampling units, with higher densities at the base of the edifice. In terms of macrofauna, high abundance of Pseudorimula midatlantica gastropods was observed at the top of the vent edifice, while numerous Ophioctenella acies ophiuroids were found at the base. Contrary to what was expected, the apparent health and abundance of mussels seems to indicate a current climax stage of the community. However, the modification of B. puteoserpentis isotopic signatures, low number of juveniles decreasing over the two years and observations made during several French cruises in the study area raise questions about the fate of the B. puteoserpentis population over time, which remains to be verified in a future sampling campaign.

Highlights

► Assemblage heterogeneity at different scales linked to fluid proximity & location. ► Meiofaunal groups dominated. Macrofaunal disparity between top and base of edifice. ► Low number of mussel juveniles over time questions the future of the population.

Please note that this is an author-produced PDF of an article accepted for publication following peer review. The definitive publisher-authenticated version is available on the publisher Web site.

Keywords : benthic ecology, associated fauna, habitat, temperature, biodiversity, hydrothermal activity, condition index, food webs, temporal variability

Please note that this is an author-produced PDF of an article accepted for publication following peer review. The definitive publisher-authenticated version is available on the publisher Web site.

1. Introduction

Hydrothermal vents sustain islands of productivity and biomass of endemic fauna (Tunnicliffe, 1991; Van Dover, 2002), thanks to the local production of organic matter by chemosynthetic microorganisms. The latter are the major primary producers of hydrothermal ecosystems as they fix inorganic carbon fueling macrofaunal communities dominated by large size taxa such as siboglinid tubeworms, provannid gastropods or bathymodiolin mussels. These large foundation species (Dayton, 1972) live in symbiosis with microorganisms with which they form functional units called holobionts (Zilber-Rosenberg and Rosenberg, 2008). These holobionts provide a substratum, a refuge as well as reproduction and feeding grounds to other smaller associated macrofaunal and meiofaunal taxa, therefore contributing to locally enhance species diversity (Goroslavskaya and Galkin, 2011; Govenar and Fisher, 2007; Sarrazin et al., 2020; Van Dover, 2002, 2003; Zekely et al., 2006). Vent faunal assemblages are patchily distributed within distinct niches

along a physico-chemical gradient from high-temperature fluid emission zones to their peripheries, according to their tolerance to environmental conditions (Tunnicliffe, 1991; Vismann, 2012) and nutritional needs (Govenar et al., 2005; Govenar and Fisher, 2007; Luther et al., 2001; Sarrazin et al., 1997, 2015). Biotic interactions also play a major role in structuring these assemblages. They include positive interactions such as facilitation (Gollner et al., 2015; Micheli et al., 2002; Mullineaux et al., 2000, 2003; Sarrazin et al., 1997) and creation of habitats by engineer species, resulting in resource sharing (Bergquist et al., 2007; Lelièvre et al., 2018; Levesque et al., 2003, 2006) and negative interactions such as predation (Hunt et al., 2004; Micheli et al., 2002), competition (Lenihan et al., 2008) and territoriality (Matabos et al., 2015). These different assemblages are strongly influenced by the environmental characteristics at the edifice and vent field scales (Sarrazin et al., 2020). Variations in abiotic conditions may in particular influence the growth conditions of microorganisms, and therefore their production and diversity (Olins, 2016; Sievert et al., 1999). Consequently, modifications of the microbial activity can trigger changes at the symbiotic compartment level, by modifying the proportion of endosymbionts and therefore, the availability of energy sources (Lutz and Kennish, 1993), which can impact the fitness of the holobionts. Foundation species may also influence the physico-chemical conditions by modifying fluid flow and composition through their 3D structure and also, the metabolic activity of their symbionts (Govenar and Fisher, 2007). Moreover, a change in the distribution and density of these engineer species may have significant effects on the composition and abundance of their associated fauna (Govenar, 2010).

Among these engineer taxa, *Bathymodiolus* spp. mytilids (Kenk & Wilson, 1985) aggregate in more or less extended patches along the Mid-Atlantic Ridge (MAR). Two symbiont-bearing species of the genus *Bathymodiolus* are found on the northern MAR: *Bathymodiolus azoricus* (800-2300m, Cosel & Comtet, 1999) dominates biological communities at Lucky Strike (LS, 37°09'N) and Menez Gwen (MG, 37°50'N) vent fields, and is present at Rainbow (36°14′N) and Lost City (30°07'N) while *Bathymodiolus puteoserpentis* (2324-3510m, Cosel, Métiver & Hashimoto, 1994) is present more south at Broken Spur (29°10'N), Snake Pit (SP, 23°22'N), Logatchev (14°45′N), Semyenov (13°31'N) and probably Irinovskoe (13°19'N) vent fields (Franke et al., 2021; Gebruk et al., 2000; Gollner et al., 2021; Maas et al., 1999; Ücker et al., 2021, Van Cosel et al., 1999). Broken Spur is a hybrid zone (O'Mullan et al., 2001) where *B. puteoserpentis* and hybrids between *B. puteoserpentis* and *B. azoricus* co-occur (Ücker et al., 2021). These two species live in symbiosis with two symbiont lineages: sulfide-oxidising (also called thiotrophic) and methanotrophic bacteria (Distel et al., 1995; Duperron et al., 2006, 2016; Fiala-Médioni et al., 2002; Fisher et al., 1993). In hydrothermal ecosystems, sulphur and methane oxidation are the main carbon fixation and energy-acquisition pathways (Conway *et al.*, 1994; Levin and Michener, 2002). Chemoautotrophic sulphur oxidizers use CO_2 as a carbon source while methane oxidizers use methane (Duperron et al., 2006), ensuring holobiont fitness in various environmental conditions. In addition, these mussels have kept the ability to

filter-feed and can exploit photosynthetic energy sources by feeding on sinking organic particles (e.g. Page et al., 1991; Piquet et al., 2022). Nevertheless, the quantity of organic matter available in the deep sea is not sufficient to sustain these mussels without the help of their symbionts (Raulfs et al., 2004). *Bathymodiolus* mussels are often colonised by *Branchipolynoe seepensis* polychaetes (Pettibone, 1986), considered either a commensal (Chevaldonné et al., 1998; Pettibone, 1986; Van Dover et al., 1999) or at least a semi-parasite (Britaev et al., 2003; Britayev et al., 2003,2007; Ward et al., 2004) species.

In the present study, we focus on *Bathymodiolus puteoserpentis* mussel assemblages from the Snake Pit (SP) vent field located on the northern MAR. At this vent field, warmer habitats host assemblages dominated by *Peltospira smaragdina* gastropods (Sarrazin et al., 2022) and *Rimicaris exoculata* shrimps (Hernández-Ávila et al., 2022; Methou et al., 2022) while *B. puteoserpentis* inhabits areas with lower hydrothermal influence. These assemblages are distributed according to their proximity to fluid emission and geomorphology of the sulfide structures. The largest known mussel assemblages of SP colonise the Moose Site (23°22'5"N; 44°56'59"W) at a depth of ~3510 meters. The structure and environmental drivers of *B. puteoserpentis* mussels have not been described in details at SP, contrary to the well-known *Bathymodiolus azoricus* assemblages found at the northernmost sites Menez Gwen, Lucky Strike and Rainbow (Husson et al., 2017; Sarrazin et al., 2015, 2020). Previous studies have shown that *B. puteoserpentis* assemblages at SP host 40 taxa, dominated by abundant copepods and nematodes (Goroslavskaya and Galkin, 2011, Zekely et al., 2006), *Ophioctenella acies* ophiuroids, *Pseudorimula midatlantica* gastropods, *Rimicaris* shrimps, and several polychaete species (Goroslavskaya and Galkin, 2011; Turnipseed et al., 2004, Zekely et al., 2006). The observed spatial heterogeneity of mussel assemblages was hypothesised to be driven by heterogeneous, fluctuating and abiotic conditions as observed for *B. puteoserpentis* assemblages at Logatchev (Zielinski et al., 2011) but these remain to be characterised at SP (Turnipseed et al., 2004). Living populations of *B. puteoserpentis* are currently known from a few vent fields (including BS, SP, Logatchev and Semyenov) and probably Irinovskoe (Gollner et al., 2021). Other populations, possibly extinct or declining, were reported at Podeba (17°08'N; (Molodtsova et al., 2017) and Logatchev-4, but these mussels were never observed at the TAG nor Ashadze vent fields. Thus, SP is currently the deepest site of the known bathymetric range of *B. puteoserpentis*. Very low recruitment rate was reported in 2001 in this field, which may suggest mussel populations living in suboptimal conditions (Turnipseed et al., 2004).

Overall, and in comparison with its northern and shallower counterpart *B. azoricus*, knowledge on population structure of *B. puteoserpentis* as well as on associated living communities remain scarce, especially regarding their temporal dynamics. In order to understand how *B. puteoserpentis* assemblages are structured in space and time, and compare our results with *B. azoricus* assemblages, we sampled *B.*

puteoserpentis assemblages in 2014 and 2018 at the Moose site at the SP vent field more than 10 years after those sampled in previous studies (Goroslavskaya and Galkin, 2011; Turnipseed et al., 2003, 2004; Zekely et al., 2006).

Our aim here is to (i) describe *B. puteoserpentis* assemblages in terms of population structure, mussel biomass and density, (ii) characterise the associated fauna and (iii) examine trophic relationships among the assemblages. In addition, we aim to identify the main environmental drivers structuring *B. puteoserpentis* communities at this site by comparing our results with those of previous studies. We hypothesise that the structure of *B. puteoserpentis* assemblages will differ according to their proximity to hydrothermal emissions, with lower specific abundance of associated fauna and higher mussel biomass in warmer habitats. From our first field observations and a previous study (Turnipseed et al. in 2004), we also hypothesise that *B. puteoserpentis* assemblages from SP may soon start to decline because of the lack of juveniles. Our study is part of a global description and comprehension of hydrothermal fauna assemblages located along the MAR, providing a dataset of their temporal evolution, testing the hypothesis of the presence of declining communities.

2. Material and methods

2.1. Study site

The Snake Pit (SP) active vent field (23°22'06"N; 44°56'59"W, 3500 m depth, Figure 1) is located on the MAR at approximately 25 km south of the Kane Fracture Zone, a deep fault that offsets the MAR left-laterally over 150 km (Durant et al., 1996; Karson et al., 1987). SP is 600 m long and 200 m wide, composed of recent hydrothermal deposits (< 4000 years, Lalou et al., 1993), and covers around 15 000 m^2 of the seafloor. The active zone is composed of several black smokers separated by slopes and hydrothermal sediment deposits (Brown and Karson, 1988; Karson et al., 1987). The active sulfide sites such as the Beehive ("Les Ruches") or Moose ("Elan") structures (Fouquet et al., 1993) host high-temperature black smoker chimneys, beehives and low-temperature diffuse emission zones as well as inactive zones (Brown and Karson, 1988).

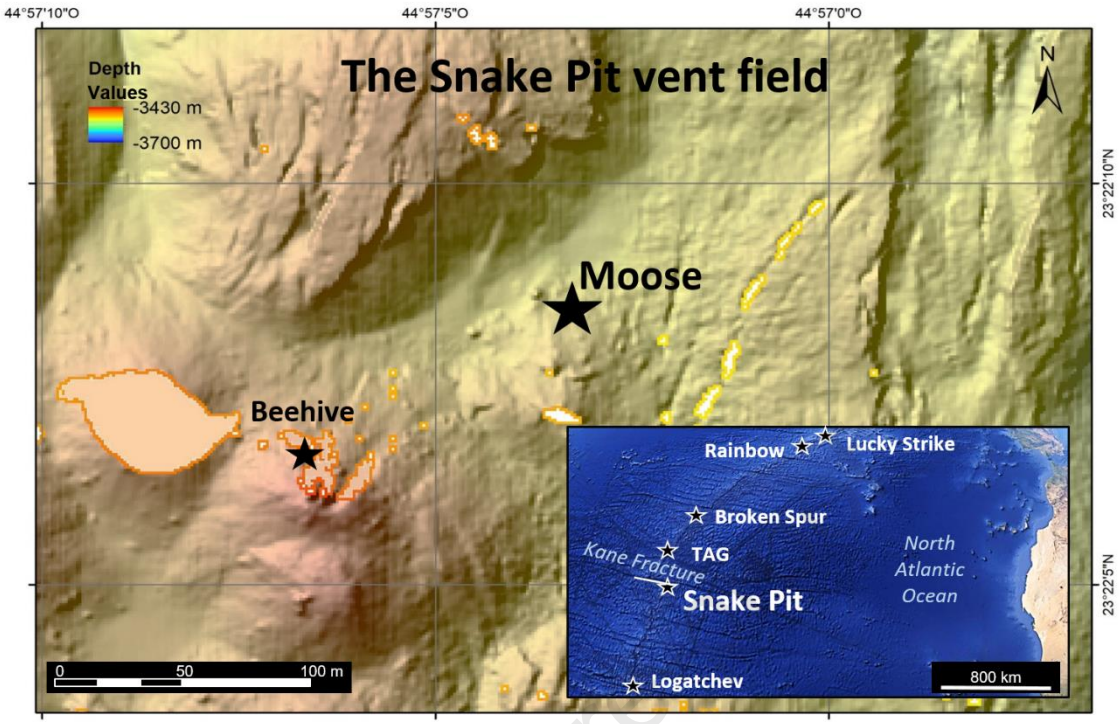

FIGURE 1. Location of the Moose sampling site (« Elan site », 23°22'.06''N; 44°56'.99''W) on the Snake Pit vent field along the Mid-Atlantic Ridge (MAR).

Snake Pit is characterised by a high mineralogical and geochemical diversity (Charlou et al., 2010). The average background seawater temperature is 2.6°C (Hernández-Ávila et al., 2022). The vent field is colonised by *Rimicaris exoculata* shrimps in the warmest areas with high sulfide concentrations (Methou et al., 2022), *Peltospira smaragdina* gastropods at intermediate temperatures and sulfide concentrations (Sarrazin et al., 2022) and *Bathymodiolus puteoserpentis* mussels in lower temperatures and hydrogen sulfide concentrations (Sarrazin et al., 2022). Our study focuses on the Moose site (23°22'5"N; 44°56'59"W, 3510 m), which occupies an area of 80 m² on the seafloor with a complex asymmetrical structure composed of active and inactive chimneys as well as beehive-shaped structures, all together resembling the antlers of a moose (Figure 2, a-c).

2.2. Characterisation of environmental conditions and faunal sampling

Environmental characterisation and sampling were done during two different cruises: a first cruise on the R/V *Pourquoi pas*? with the ROV Victor6000 in 2014 (BICOSE 1, DOI: https://doi.org/10.17600/14000100) and a second cruise in 2018 (BICOSE 2, DOI: http://dx.doi.org/10.17600/18000004) with the same research vessel but with the manned submersible Nautile. Mussel assemblages were sampled on the Moose site Figure 2 a-c). For each year, three 27 cm-long calibration targets CASIMIR were deployed on top of the mussels in order to visually estimate the

distance between sampling units (SUs) thanks to visible 7 x 7 mm checkerboards. In 2014, these targets were placed directly on *B. puteoserpentis* assemblage located at the top of the edifice, approximately thirty centimetres from each other (Figure 2 d), defining three sampling areas (SU-1, SU-2, SU-3, Table 1). In 2018, these CASIMIR targets were placed on a mussel assemblage at the base of the same edifice, spaced by approximately one metre (Figure 2 e-g), defining three additional sampling areas (SU-4, SU-5, SU-6, Table 1). Moreover, in 2014 only, each CASIMIR was equipped with autonomous MISO probes to measure variations of *in situ* temperatures directly above the mussels (few cms) during 4 days and 14 hours (MISO New, Low-T Logger Manual, precision: +/- 0.22°C at 25°C, measurement frequency: 30 s).

The *in situ* chemical analyser CHEMINI (Vuillemin et al., 2009) was used to characterise sulfide and iron concentrations with sampling probes directly above the fauna (few cms) near each CASIMIR target. The submersible temperature sensor, associated with the sampling cannula of the CHEMINI, provided temperature conditions from which we calculated the mean, minimum and maximum. The *in situ* water samplers PEPITO (2014), PIF (2018) and PLUME (2018) designed for the Nautile sampling, collected fluids directly above the fauna for subsequent chemical analyses in the laboratory. pH was measured on fluid samples upon arrival on board. Fe^{2+} values and methane concentrations (obtained from water samples) were only obtained from a single sampling unit, SU-3 for Fe^{2+} and SU-1 for methane and therefore do not appear in Table 1.

Journal Pre-proof

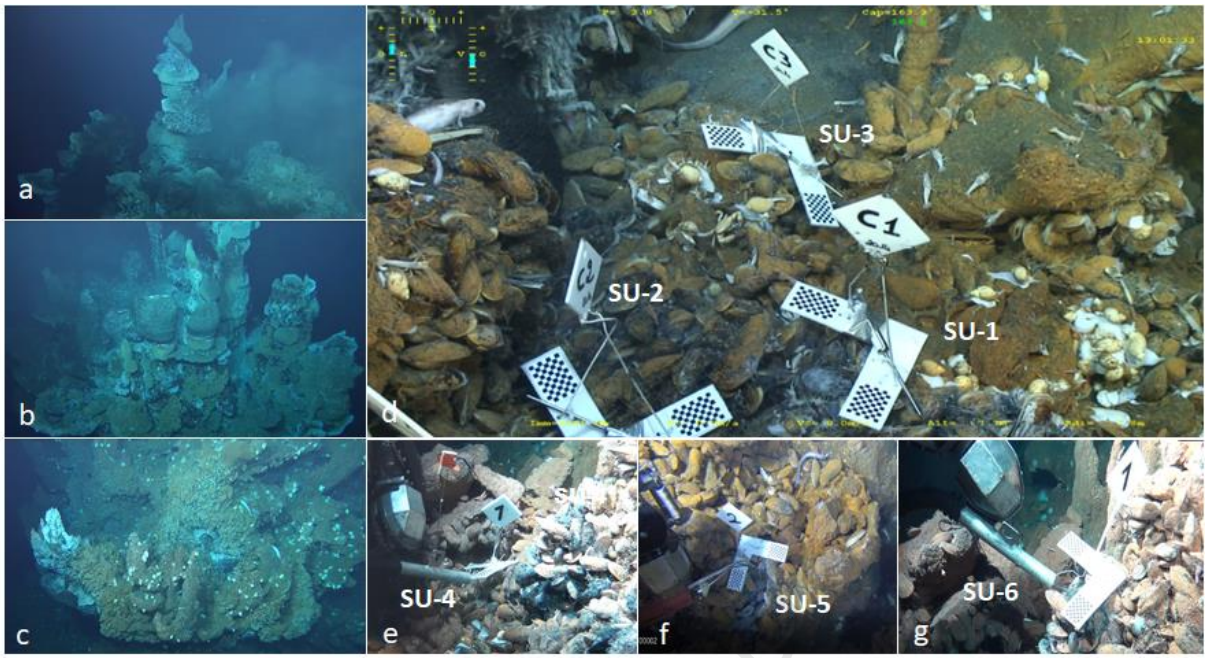

FIGURE 2. Sampling of mussel assemblages on the Moose edifice on the Snake Pit vent field. Left (a-b-c) : large views of the Moose edifice taken with the 4K camera of the Nautile showing the top (a), the global structure (b) and the base (c) of the sulphide edifice. (d) Sampling sites during BICOSE 2014 (*"CASIMIR C1"* corresponds to the sampling unit SU-1, *"CASIMIR C2"* corresponds to SU-2, *"CASIMIR C3"* corresponds to SU-3). (e-f-g) Sampling sites during BICOSE 2018 (*CASIMIR 1* (e) corresponds to SU-4, *CASIMIR 2* (f) corresponds to SU-5, *CASIMIR 1* (g) corresponds to SU-6).

After the environmental characterization, the mechanical arms of the submersibles meticulously removed the mussels and their associated fauna, and placed them in small isotherm sampling boxes. Sampling was completed using the submersible suction samplers to account for the smaller and/or mobile fauna (see sampling protocol in Sarrazin et al., 2015) on all SUs except SU-1 and SU-2 (Table 1). Environmental data are summarised in Tables 1 & 2.

Mussel assemblage	Year	Dive	PBT	SS	T°C mean (std)	T°C max	T°C min	T°C range	T°C anomaly	pH	H_2S (std) (µM)	Fe_{total} (std) (µM)
SU-1	2014	565-02	✓	X	4.3 (0.9)	9.3	2.2	7.1	1.7	8	10.2 (4)	-
SU-2	2014	565-02	✓	X	2.7 (0.2)	4.0	2.2	1.8	0.1	-	0.4 (0.2)	-
SU-3	2014	565-02	✓	✓	2.6 (0.1)	3.1	2.3	0.8	0	-	0.7 (0.2)	-
SU-4	2018	1922-16	✓	✓	3.2 (0.1)	3.6	3.0	0.6	0.6	7.8	n.d.	4.4
SU-5	2018	1922-16	✓	✓	4.2 (1.3)	6.9	2.6	4.3	1.6	7.5	n.d.	12.3
SU-6	2018	1922-16	✓	✓	4.3 (1.3)	6.9	2.6	4.3	1.7	7.6	n.d.	13.2
TOP	2014	565-02			3.2 (1)	5.5 (3.4)	2.2 (0.1)	3.2 (3.4)	0.6 (1)	8	3.8 (5.6)	-
BASE	2018	1922-16			3.9 (0.6)	5.8 (1.9)	2.7 (0.2)	3.1 (2.1)	1.3 (0.6)	7.6 (0.2)	n.d.	10 (4.8)

Table 1. Sampling characteristics and physico-chemical conditions in the two *Bathymodiolus puteoserpentis* mussel assemblages studied in 2014 and 2018 on the Moose site from the Snake Pit vent field (Mid-Atlantic Ridge). PBT: small boxes used for faunal sampling. SS: suction samplers used for faunal sampling. The green check mark and the red cross indicate the use or not of the corresponding sampling method. Temperatures (T°C) were obtained by submersible probes (mean + standard deviations). Ranges were calculated by the difference between the maximum and minimum temperatures. Temperature anomalies were obtained by subtracting the established background temperature of 2.6°C at this field (Hernàndez-Avila et al., 2022) from the measured temperatures. Other parameters (pH, H_2S: concentrations of hydrogen sulfide, Fe: concentrations of iron) were obtained by CHEMINI and water sampling tools PEPITO (2014) and PIF/PLUME (2018). The three H_2S concentrations measured in 2018 were below the detection threshold n.d.). TOP corresponds to the average of the values measured in 2014 at the top of the edifice (SU-1, SU-2, SU-3). BASE corresponds to the average of the values measured in 2018 at the edifice's base (SU-4, SU-5, SU-6). Standard deviations are given in parenthesis.

Mussel assemblage	T°C mean (std)	T°C max	T°C min	T°C range
SU-1	6.6 (2.3)	15.8	2.6	13.2
SU-2	3.8 (0.8)	7.5	2.4	5.0
SU-3	2.9 (0.2)	3.7	2.5	1.2

Table 2. Time-series of temperature (T°C) means, standard deviations (std), maximum (max), minimum (min) and range over the *Bathymodiolus puteoserpentis* mussel assemblage located at the top of the Moose edifice (2014) from the Snake Pit vent field (Mid-Atlantic Ridge). These temperature time-series were recorded by MISO probes from 18/01/2014 to 22/01/2014.

2.3. Faunal analyses

On board, mussel individuals were isolated, briefly opened and preserved in 5-litre containers filled with 4% formalin. The rest of the faunal sample (sampling box + suction sampler when performed) was sieved on 300 µm and 20 µm meshes. Large individuals of the 300 µm fraction were picked and 109 individuals (47 in 2014, 62 in 2018), representing key macrofaunal species, were conditioned at -80°C for isotopic analyses and barcoding. The remaining fauna from the 300 µm-fraction was preserved in 96% ethanol and that of the 20 µm-fraction (meiofauna) in 4% formalin for subsequent identification in the lab.

2.3.1 Mussel biomass & volume

Mussel biomass and volumes were evaluated for each sampling unit to provide a standardisation mean and allow comparison between samples and other studies. After rinsing with water and draining, each mussel individual was measured (length, width, thickness) using an electronic caliper. The wet weight (WW) was evaluated by weighing whole organisms in aluminum cups and also, the shells and flesh separately. Then, the cups were placed in a 60°C oven for 48 hours in order to eliminate water and obtain the dry weight (DW) that contains both the organic and inorganic materials. Finally, dry tissues were placed in a 550°C oven for seven hours to remove the organic part and obtain the ash weight (AW). The ash-free dry weight (DW – AW = AFDW) corresponds to the quantity of organic matter in the sample. However, two very small individuals were too difficult to open and were not considered in the calculation of biomass. For these

individuals, only morphometric measurements were performed. Missing morphometric or biomass values (NA) in the global dataset -due to small size or sometimes broken shells-, were replaced (~8% of the data), thanks to the missMDA R package. An iterative Principal Component Analysis (PCA) was used to replace NAs with coherent and non-random data. To standardise our sampling units, two metrics were used: (1) the estimated area provided by the mussels (m^2) for each SU, calculated by summing the area provided by each individual mussel shell, considering these as being flat ellipsoids (area of two elliptical surfaces $=2(a \times b \times \pi)$ with $a = length/2$ and $b = width/2$), (2) the estimated volume occupied by the mussels (dm^3) for each SU, calculated by summing the volume occupied by each mussel (ellipsoid volume $= \frac{4}{3}\pi \times a \times b \times c$, with $a = length/2$; $b = width/2$; $c = thickness/2$ (Table 3). Moreover, condition index (CI) of each mussel was estimated with the ratio $CI = W/V$ $with$ $W = AFDW$ $(g) =$ $organic\ matter$ and $V = shell\ volume$ (mL), with the aim of comparing the general physiological condition of individuals between samples and location on the Moose edifice (Table 3). CI is a well-accepted method of determining the physiological condition of bivalves (Fisher et al., 1988; Lenihan, 1999; Lenihan et al., 2008; Smith, 1985).

2.3.2 Identification of the associated fauna

Once in the lab, all macrofaunal individuals (>300 µm) were picked individually from each of the sampling units and identified to the lowest taxonomic level possible using a binocular magnifier. To facilitate sorting, all meiofaunal individuals (from the 20 µm and >300 µm fractions) were transferred separately to a small volume of 96% ethanol, stained with Phloxine B, which colours the organic matter in pink, and rinsed. For them, taxonomic identification was carried out at higher taxonomic levels (order/class). All fauna (both sieves) belonging to Nematoda, Copepoda and Halacaridae were considered as meiofauna. Juveniles of macrofauna found in the lower 20 µm fraction were considered as macrofauna.

2.3.3 Isotopic analyses

Stable isotope ratios of carbon ($^{13}C/^{12}C$ or $\delta^{13}C$) and nitrogen ($^{15}N/^{14}N$ or $\delta^{15}N$) were used to describe food-web structure and characterise trophic interactions of mussels and their associated fauna. It is accepted that in natural environments, $\delta^{13}C$ can be used to identify the food sources and remains relatively unchanged between successive trophic levels, ~1‰ between each trophic level (DeNiro and Epstein, 1978). The $\delta^{13}C$ of local primary producers depend on the isotopic values of their carbon sources and their isotopic fractionation during carbon fixation (Portail et al., 2018). This includes autotrophs using the Calvin-Benson-Bassham (CBB) cycle or the reducing tricarboxylic acid (rTCA) cycle as well as methanotrophs. $\delta^{15}N$ is a good indicator of trophic position: successive trophic levels become enriched in $\delta^{15}N$ for approximately 3.4‰ per trophic level (Minagawa and Wada, 1984) or more generally between 2 and 4‰

(McCutchan et al., 2003). Both isotopic ratios are expressed according to the δ notation in ‰ (Coplen, 2011), in reference to the international references Atmospheric Air for nitrogen and Vienna Pee Dee Belemnite for carbon.

Isotopic ratios of carbon and nitrogen were determined on 47 individuals belonging to 10 species in 2014 and 62 individuals belonging to 4 species in 2018. The treatment varied according to the taxa. Organisms were dissected to keep their muscles, or, when body size was small, the whole organism was used (Mateo et al., 2008). Some mussels hosted *Branchipolynoe seepensis* polynoids in their mantle cavity: those were isolated and measured. Samples were placed in the oven at 50°C during 48h before being ground in a homogeneous powder using mortar and pestle. Samples containing hard inorganic carbon parts that could not be physically removed (copepods) were conditioned in silver capsules and were decalcified with hydrochloric acid to remove carbonates from their exoskeleton. When possible, isotopic analyses were done on several individuals per taxon in order to take into account intraspecific variability. Stable isotope ratio measurements were performed via continuous flow- elemental analysis - isotope ratio mass spectrometry (CF-EA-IRMS) at University of Liège (Belgium), using a vario MICRO cube C-N-S elemental analyzer (Elementar Analysensysteme GMBH, Hanau, Germany) coupled to an IsoPrime100 isotope ratio mass spectrometer (Isoprime, Cheadle, United Kingdom). IAEA (International Atomic Energy Agency, Vienna, Austria) certified reference materials sucrose (IAEA-C-6; $\delta^{13}C = -10.8 \pm 0.5‰$; mean ± sd) and ammonium sulfate (IAEA-N-2; $\delta^{15}N = 20.3 \pm 0.2‰$; mean ± sd) were used as primary analytical standards. Sulfanilic acid (Sigma-Aldrich; $\delta^{13}C = -25.6 \pm 0.4‰$; $\delta^{15}N = -0.13 \pm 0.4‰$; mean ± sd) was used as a secondary analytical standard. Standard deviations on multi-batch replicate measurements of secondary and internal lab standards (amphipod crustacean muscle) analysed interspersed with samples (one replicate of each standard every 15 analyses) were 0.2‰ for both $\delta^{13}C$ and $\delta^{15}N$.

2.3.4 Statistical analyses

All analyses were computed with R (v. 4.2.1, R Core Team, 2022).

Mussel population- The number of mussels analysed for their sizes varied between 18 to 52 and those analysed for their biomass varied between 18 to 51 (Table 3). Mussel biomass and abundance data were pooled by sampling year and compared with the Wilcoxon-Mann-Whitney (WMW) non-parametric test, on three main parameters: shell length, dry weight (DW) and ash-free dry weight (AFDW). Then, a multi-comparison of the six sampling units was done with a Kruskal-Wallis test.

Alpha diversity- As they represent the structuring species, *Bathymodiolus puteoserpentis* mussels were not taken into account in the statistical analyses of the associated fauna. Standardised to surface mussel area or estimated volume, associated fauna abundance datasets were subjected to several statistical tests in order to

evaluate their similarity with the WMW and Kruskal-Wallis (KW) tests, completed when necessary by a Post Hoc Dunn's test. Alpha diversity of each sample was assessed through two indices: the Shannon-Wiener's diversity index (H') which takes into account species richness and the relative abundance of species with a sensitivity to rare species. H' can vary between 0 (absence of diversity) and to a H max that is dataset dependent (high diversity). The Piélou evenness index (J') characterises the homogeneity of a community. It varies between 0 in a community with only one species, and 1 in a community where all species have equal relative abundance.

Beta diversity- Then, in order to compare the two mussel assemblages (2014 at the top of the edifice, 2018 at the base) and especially their associated fauna, the β-diversity was assessed with a PCA with Hellinger transformation on the associated fauna dataset. The comparison analyses of the associated fauna were carried out both by including all the individuals collected (sampling boxes and suction sampling), but also by excluding the individuals recovered by suction sampling for a homogenised comparison of SUs. The relative abundance trends observed being the same, the results presented below include all individuals collected, all methods combined.

3. RESULTS

3.1. Physico-chemical conditions

3.1.1. Point temperature measurements- Higher average temperatures were recorded at SU-1, SU-5 and SU-6 (Table 1). SU-1 also exhibited the highest maximal temperatures, as well as the higher variability (7.1°C). SU-2, SU-3 and SU-4 exhibited the lowest and more stable temperatures.

3.1.2. Temperature dynamics- In 2014, the MISO probes continuously measured the temperatures on the three sampling units (See Supplementary materials, Figure S1). Mean temperatures were 6.6 ± 2.3°C on SU-1, 3.8 ± 0.8°C on SU-2 and 2.9 ± 0.2°C on SU-3 (Table 2). At the start of the deployment, the temperature values varied between 3-4°C while at the end of the deployment, they did not exceed 3°C in all SUs. A peak in temperature reaching 15.8°C was recorded on SU-1 after 3 days of measurements, dropping rapidly to ~7°C a few minutes later. The other two SUs showed lower temperature variations.

3.1.3. Physico-chemical measurements- The pH values were slightly lower for the SUs sampled in 2018 than for SU-1 (Table 1). pH values at sites SU-2 and SU-3 were missing. Mean H_2S concentrations reached 10.2 µm in SU-1, which was higher than in all other samples. In 2018, values of Fe_{Total} were similar in SU-5 and SU-6 and three times higher than those recorded in SU-4 (Table 1). Fe^{2+} values (*in situ*) showed an average of 32.2 ± 7.5 µM on SU-3 (not presented in the table). Similarly, methane concentrations reached 0.33 µM for SU-1 (0.33 µM, not presented in the table). Due to these discrepancies in environmental data

acquisition, only temperature variables were used to compare the SUs, the other factors being presented for discussion purposes.

3.2. Habitat description- The habitat of the 2014 samples, located at the top of the Moose edifice, was characterised by the presence of an important aggregate of *Rimicaris* shrimps with few *Pachycara thermophilum* zoarcid fishes, *Segonzacia mesatlantica* crabs and *Phymorhynchus* gastropods. At SU-1 and SU-2, the mussels densely covered the edifice surface, forming a thick layer of stacked mussels, thus impairing proper evaluation of the surfaces sampled through imagery. At SU-3 however, the assemblage was less thick and the greyish rocky substratum was apparent. The habitat of the 2018 samples, at the base of the edifice, was characterised by dense mussel assemblages, colonising orange and greyish substrata. A few individuals of *P. thermophilum* and *Phymorhynchus* gastropods were observed. None to rare filamentous microbial mats were observed near the sampling areas during the two cruises. Contrary to what was expected, mean temperatures were quite similar in the mussel assemblages from the top and base of the edifice despite small scale heterogeneity. However, the closer proximity to fluid emissions of sampling units at the top of the edifice is reflected in the higher hydrogen sulfide concentration measured at SU-1.

3.3. *Bathymodiolus puteoserpentis*: population size structure and biomass analyses- Overall, mussel lengths varied between 5.5 mm and 125.2 mm, with an average length of 84.06 ± 24.01 mm. When data were pooled by sampling year, Wilcoxon-Mann-Whitney (WMW) non-parametric test showed that the median shell lengths did not vary significantly between 2014 (82.81 ± 27.15 mm) and 2018 (85.41 ± 20 mm, p-value of 0.92). Nevertheless, Kruskal-Wallis test showed that the mean shell lengths varied significantly between SUs (p-value of 9.27e-09), and post hoc Dunn's test indicated that those for SU-1 were significantly higher from those of SU-2 and SU-6 (Table 3). Mean shell lengths of SU-2 were significantly smaller than all other SUs, except SU-6 (Table 3). The mean lengths of the four remaining SUs did not differ significantly from each other. The most represented shell sizes were found in the 50-115

328 mm interval. All mussels were larger than 15 mm, except for SU-2 and SU-6, which both included one
329 specimen below 15 mm (Figure 3).

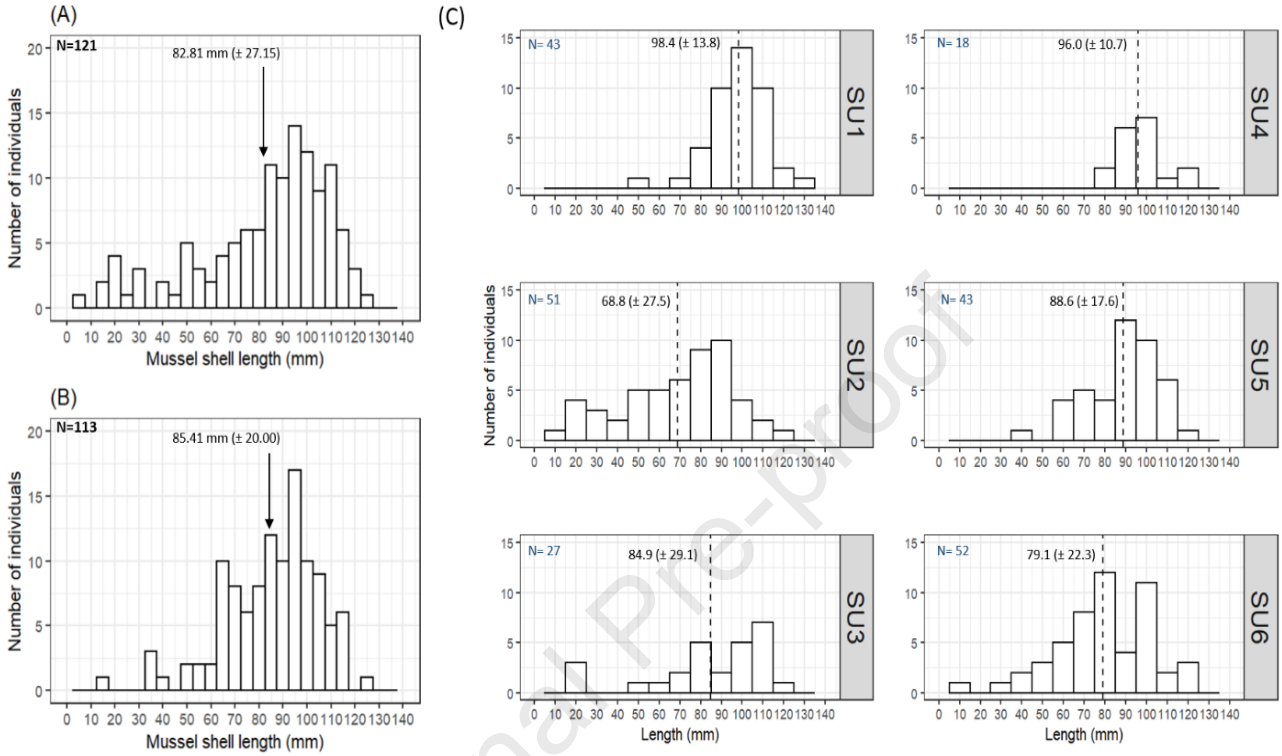

FIGURE 3. Size-frequency structure of *Bathymodiolus puteoserpentis* mussels sampled (A) in 2014 and (B) in 2018 during the BICOSE cruises and (C) both years by sampling units on the Moose site at the Snake Pit vent field (Mid-Atlantic Ridge). "N" corresponds to the number of mussels in good condition that could be measured by cruise/by sampling unit. Arrows indicate the average lengths of mussel shells and with standard deviations in parentheses. The size unit in mm was chosen to facilitate comparison with the size structure of *B. puteoserpentis* established by Won *et al.*, 2003a on the Logatchev vent field.

330
331
332

Journal Pre-proof

Journal Pre-proof

										With meiofaunal taxa			Without meiofaunal taxa		
Sampling units	**N mussel (morpho/biomass)**	**N mussel (total)**	**Mean WW (g)**	**Mean DW (g)**	**Mean AFDW (g)**	**Mean shell length (mm)**	**Total area (m^2)**	**Total volume (L)**	**CI (g/mL)**	**N taxa**	**H' index**	**J' index**	**N taxa**	**H' index**	**J' index**
SU-1	43	43	**20.1** (±5.7)	**4.0** (±1.3)	**3,6 (±1.2)**	**98.4 (±13.8)**	**0.31**	**4.00**	**0.039** (+0.009)	9	**1.35**	**0.62**	7	0.93	0.48
SU-2	**52***	**60**	11.5 (±7.5)	2.0 (±1.2)	1,7 (±1.2)	68.8 (±27.5)	0.26	2.80	0.038 (+0.009)	12	1.26	0.51	9	1.49	0.68
SU-3	27	33	17.2 (±9.8)	2.4 (±1.4)	2,3 (±1.3)	84.9 (±29.1)	0.20	2.34	0.033 (+0.006)	12	0.98	0.40	9	1.34	0.61
SU-4	18	23	14.8 (±3.8)	2.2 (±0.7)	2,0 (±0.7)	96.0 (±10.7)	0.16	1.90	0.025 (0.006)	13	1.22	0.48	10	0.58	0.25
SU-5	43	49	14.5 (±6.9)	2.6 (±1.3)	2,4 (±1.2)	88.6 (±17.6)	0.30	3.65	0.032 (+0.008)	**14**	1.02	0.39	**11**	0.76	0.32
SU-6	**52***	58	13.2 (±8.3)	2.5 (±1.7)	2,3 (±1.6)	79.08 (±22.3)	0.30	3.39	**0.039** (+0.012)	12	0.75	0.30	9	**1.56**	**0.71**
TOP	**122***	**136**	**15.8** (±8.4)	**2.8** (±1.5)	**2,5** (±1.5)	82.8 (±27.2)	**0.78**	**9.30**	**0.037** (+0.009)	16	**1.37**	**0.50**	13	**1.54**	**0.60**
BASE	113*	130	13.9 (±7.2)	2.5 (±1.4)	2,3 (±1.3)	**85.4** (±20.0)	0.75	8.89	0.034 (+0.011)	16	0.93	0.33	13	0.93	0.36

Table 3. Morphometric and biomass characteristics of *Bathymodiolus puteoserpentis* mussels as well as diversity of associated fauna sampled in 2014 and 2018 on the Moose Site from the Snake Pit vent field (Mid-Atlantic Ridge). N morpho/biomass: number of mussels measured and analysed for biomass. N total: total number of mussels sampled, including those used in isotopic analyses. Mean WW: mean wet weight. Mean DW: mean dry weight. Mean AFDW: mean ash-free dry weight = total organic matter. Shell length (mm) = corresponds to the average shell length of mussels. Estimated areas in m^2 were calculated by summing individual areas of each mussel and corresponds to the colonisation surface offered by the mussels (see M&M section). Estimated volumes in L were calculated by summing individual volumes of each mussel (see M&M section). CI: average condition index of the mussels in the SU. N taxa: number of associated fauna taxa (not including *B. puteoserpentis*). H' corresponds to the Shannon's diversity index, J' corresponds to the Piélou's evenness index, both indexes were calculated with and without meiofauna.*: one small individual not included in biomass measurements. Higher values are highlighted in bold.

Overall, mussel's mean individual wet, dry and ash free dry weights varied between sampling units (Table 3). The quantity of organic matter (AFDW, Table 3) varied from 1.7 ± 1.2 g and 3.6 ± 1.2 g. A Kruskal-Wallis test showed that the AFDW varied significantly between SUs (p-value of 9.84 e-09), and post hoc Dunn's tests indicated that it was significantly higher on SU-1 than all others (Table 3). The condition index was also significantly higher on SU-1 than those of SU-3, SU-4 and SU-5 (Table 3).

3.4. Composition and abundance of the associated fauna

A total of 23,207 individuals were sorted: 1885 in the macrofaunal and 21,322 in the meiofaunal (copepods, nematodes, Halacaridae, 20 µm and 300 µm) compartments. Overall, meiofaunal taxa dominated the fauna associated with *Bathymodiolus puteoserpentis* mussel assemblages in terms of relative abundance in all SUs except SU-1 where they represented less than 44% of all sorted individuals (Figure 4, Table 4). Nematodes dominated the meiofauna of all SUs except SU-1 and to a lesser extent SU-5, both dominated by copepods. Macrofaunal taxa were dominated by the limpet *Pseudorimula midatlantica* in sampling units from the top of the edifice in 2014 (from 42.4% to 73.8% of the macrofaunal abundance), while it was almost absent in the sampling units from the base in 2018 (<1.5% of the macrofaunal abundance; Figure 4).

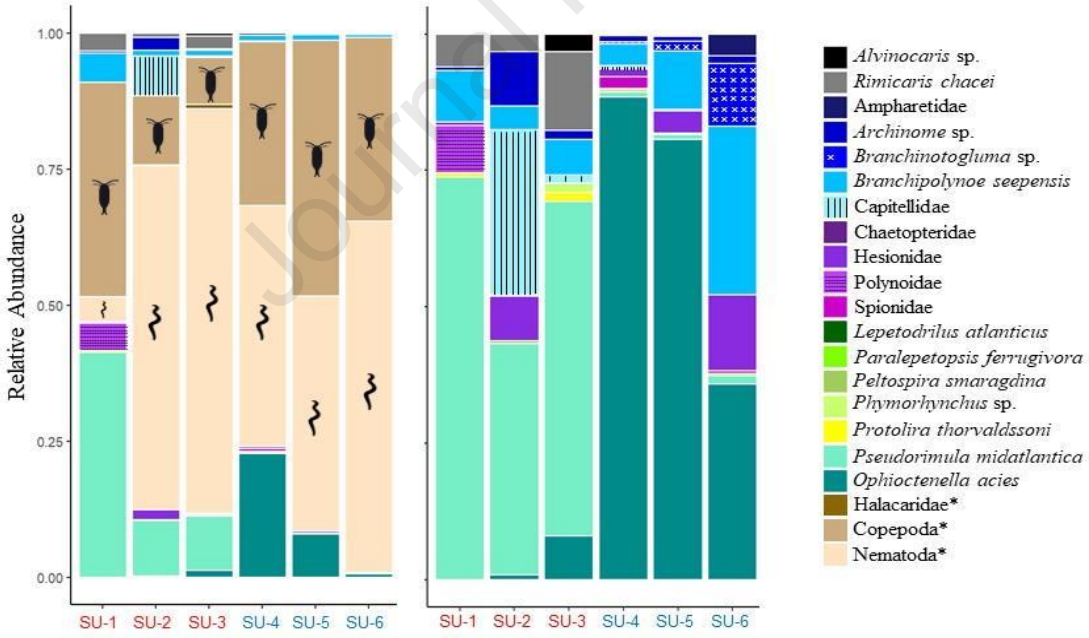

FIGURE 4. Stacked bar graphs showing the composition of associated fauna in *Bathymodiolus puteoserpentis* mussel assemblages sampled on the Moose site at the Snake Pit vent field during the BICOSE cruises (SU-1, SU-2, SU-3 in red for 2014, SU-4, SU-5, SU-6 in blue for 2018). *The left bar graph includes Copepoda, Halacaridae, Nematoda while the right one excludes them for better reading.

Journal Pre-proof

Conversely, the ophiuroid *Ophioctenella acies* dominated the edifice's base with abundances varying from 35.8% to 88.5% of the total macrofaunal abundance while only a few individuals were found at the top. Densities of associated fauna (macro- and meiofauna) were higher in samples from the base than those from the top of the edifice (Table 4).

Phylum Class	Family	Taxa	SU-1	SU-2	SU-3	SU-4	SU-5	SU-6
			Relat. Ab %	Relat. Ab %	Relat. Ab %	Relat. Ab %	Relat. Ab %	Relat. Ab %
Annelida								
Polychaeta	Ampharetidae		0.00	0.00	0.00	0.08	0.03	0.07
	Amphinomidae	*Archinome* sp.	0.38	2.39	0.26	0.31	0.09	0.03
	Capitellidae		0.00	7.25	0.26	0.16	0.03	0.00
	Chaetopteridae		0.00	0.06	0.00	0.00	0.00	0.00
	Hesionidae		0.38	1.94	0.00	0.39	0.41	0.24
	Polynoidae		4.89	0.00	0.00	0.00	0.00	0.00
	Polynoidae	*Branchinotogluma* sp.	0.00	0.00	0.00	0.08	0.18	0.19
	Polynoidae	*Branchipolynoe seepensis*	5.26	1.04	1.05	1.01	1.05	0.52
	Spionidae		0.00	0.00	0.00	0.55	0.01	0.01
Arthropoda								
Arachnida	*Halacaridae		0.00	0.06	0.79	0.08	0.03	0.03
***Copepoda**			**39.47**	12.75	8.64	**30.05**	**46.92**	**33.76**
Crustacea	Alvinocarididae	*Alvinocaris* sp.	0.00	0.00	0.52	0.00	0.00	0.00
		Rimicaris chacei	3.38	0.78	2.36	0.00	0.01	0.00
Echinodermata								
Stelleroidea	Ophiuridae	*Ophioctenella acies*	0.00	0.19	1.31	**22.72**	7.91	0.61
Mollusca								
Gastropoda	Lepetodrilidae	*Lepetodrilus atlanticus*	0.00	0.00	0.00	0.00	0.01	0.00
		Pseudorimula midatlantica	**41.35**	10.16	9.95	0.23	0.09	0.03
	Neolepetopsidae	*Paralepetopsis ferrugivora*	0.00	0.00	0.00	0.00	0.00	0.01
	Peltospiridae	*Peltospira smaragdina*	0.00	0.13	0.00	0.00	0.00	0.00
	Raphitomidae	*Phymorhynchus* sp.	0.00	0.00	0.26	0.16	0.00	0.00
	Skeneidae	*Protolira thorvaldsoni*	0.38	0.00	0.26	0.00	0.00	0.00
***Nematoda**			4.51	**63.24**	**74.35**	**44.18**	**43.24**	**64.51**
Total number of individuals (*considered as meiofauna)			266	1545	382	1281	7886	**11847**
Total relative abundance meiofauna (%)			43.98	76.05	83.78	74.31	90.19	**98.3**
Total relative abundance macrofauna (%)			**56.02**	23.94	16.23	25.69	9.82	1.71

Table 4. Relative abundances of associated fauna sampled in mussel assemblages on the Moose Site of the Snake Pit vent field (Mid-Atlantic Ridge) in 2014 and 2018. *Copepoda, Halacaridae and Nematoda are considered as meiofauna (coming from the 20 µm and 300 µm fractions, see M&M). Higher values are highlighted in bold.

Overall, 21 taxa (Class/family/species) were identified across all samples, including 18 for macrofauna (family/species). Total taxonomic richness varied from 9 in SU-1 to 14 in SU-5 (Table 3). SU-1 exhibited a co-dominance of *Pseudorimula midatlantica* (41.3%) and copepods (39.5%), as well as other taxa in relatively significant abundance (undetermined polynoids, *B. seepensis*, *Rimicaris chacei*, and nematodes) which contributed to the highest diversity indexes found in this sample despite its lowest number of taxa (Table 3). SU-4 and SU-5 harboured a co-dominance of copepods and nematodes, with highest abundance of *O. acies* in the macrofaunal compartment. These two SUs had no other well-represented taxa in terms of abundance, as illustrated by their overall lower diversity index values than SU-1. Although it exhibited more taxa, many of which contributed in very low proportions to the total abundance. The other SUs were rather

characterised by a strong dominance of nematodes. SU-2 and SU-3 were similar in terms of abundance. SU-6 harboured lower diversity and evenness indexes linked to the very low representation of taxa other than nematodes and copepods (Table 3). Nevertheless, the diversity is generally low in each of the sampling units, whether we are interested in species richness or diversity indexes.

A total of seven polychaete families were found (in addition to a few undetermined ones of poor condition). They were particularly abundant in samples from the base of the edifice representing from 10% to 63% of the macrofaunal abundance in SU-4 and SU-6 respectively. They include Ampharetidae, *Branchinotogluma* sp. and Spionidae. *Branchipolynoe seepensis* polychaetes were more abundant in samples from the base, representing from 4% to 31% of the macrofaunal abundance in SU-4 and SU-6 respectively. A high abundance of Capitellidae (30.3%) and to a lesser extent *Archinome* sp. (10%) polychaetes were found in SU-2. Alvinocaridid shrimps (*Rimicaris chacei*, *Alvinocaris markensis*) were found almost exclusively in samples from the top of the edifice. Similarly, the small gastropods *Peltospira smaragdina* and *Protolira thorvaldssoni* were only recorded from the top of the edifice although in low numbers. Two other gastropod species (*Lepetodrilus atlanticus* and *Paralepetopsis ferrugivora*) were found in low abundance, but at the base. Finally, *Phymorhynchus* sp. was present in two out of six samples.

According to the PCA on macrofaunal taxa, the first component explained 37.7% of the distribution of the fauna. SU-1, SU-2 and SU-3 are positively loaded on the first component, while SU-4, SU-5 and SU-6 are negatively loaded on the first component, showing a clear distinction between the samples from the top to those from the base of the edifice, supporting the observed differences in community structure (Figure 5). The PCA showed also similarities between SU-1 and SU-3, probably due to their low faunal abundances (with the exception of several polychaetes and shrimps) and diversities and between SU-5 and SU-6 which exhibited similar macrofaunal dominance (*O. acies*, *Branchipolynoe seepensis*). The second component explains 28.6% of faunal distribution.

Journal Pre-proof

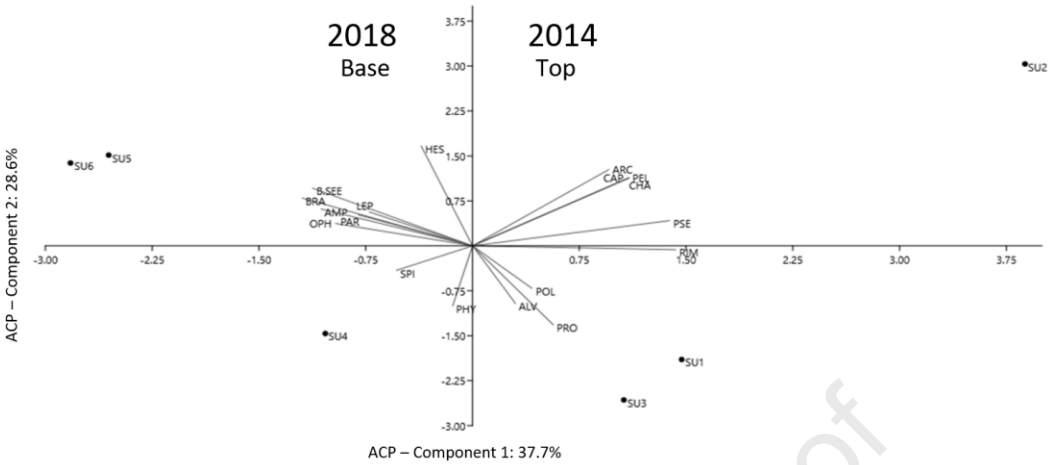

FIGURE 5. Principal component analysis (PCA) of macrofaunal individuals associated to *Bathymodiolus puteoserpentis* mussel assemblages from the Moose site from the Snake Pit vent field (Mid-Atlantic Ridge). Meiofauna (including nematodes, copepods and halacarids) have been removed from the analysis for better graphical reading. The component 1 explains 37.7% in faunal distribution showing a clear separation between the assemblages sampled in 2014 (right side) and those sampled in 2018 (left side). Axis 2 explains 28.6% in faunal distribution. ALV: *Alvinocaris chacei;* AMP: Ampharetidae; ARC: *Archinome sp.*, ; B.SEE: *Branchipolynoe seepensis*; BRA: *Branchinotogluma sp.*; CAP: Capitellidae; CHA: Chaetopteridae; HES: Hesionidae; LEP: *Lepetodrilus atlanticus*; OPH: *Ophioctenella acies*; PAR: *Paralepetopsis ferrugivora*; PHY: *Phymorhynchus sp.*; PEL: *Peltospira smaragdina*; POL: Polynoids; PRO: *Protolira thorvaldssoni*; PSE: *Pseudorimula midatlantica*; RIM: *Rimicaris chacei*; SPI: Spionidae.

3.5. Isotopic analyses

Bathymodiolus puteoserpentis mussels were distributed in two groups (Figure 6). The first one, which included most of the mussels (90%), showed $\delta^{13}C$ values ranging from -35.64‰ to -31.09‰ and $\delta^{15}N$ values ranging from -15.42‰ to -4.83‰. The second group included only three mussels from the base of the edifice with much higher values ranging between -16.35‰ to -12.73‰ for $\delta^{13}C$ and +4.53‰ to +7.10‰ for $\delta^{15}N$. *Branchipolynoe seepensis* polychaetes exhibited isotopic values very close to those of *B. puteoserpentis*, ranging between -34.9‰ to -11.1‰ for $\delta^{13}C$ and from -15.4‰ to +8.9% for $\delta^{15}N$ (Figure 6). However, a few of them differed and appeared to be independent of the mussels. *Ophioctenella acies* isotopic ratios were much less spread than those of *B. seepensis* and *B. puteoserpentis*, and were grouped between -26.5‰ and -22.6‰ for $\delta^{13}C$ (with an outlier of -12.5‰) and between -4.6‰ and +1.3‰ for $\delta^{15}N$ (with an extreme value of 6.4‰) (Figure 6). Only three ophiuroids sampled in 2014 were analysed, against 24 for 2018, giving similar results for $\delta^{13}C$ values but higher $\delta^{15}N$ values.

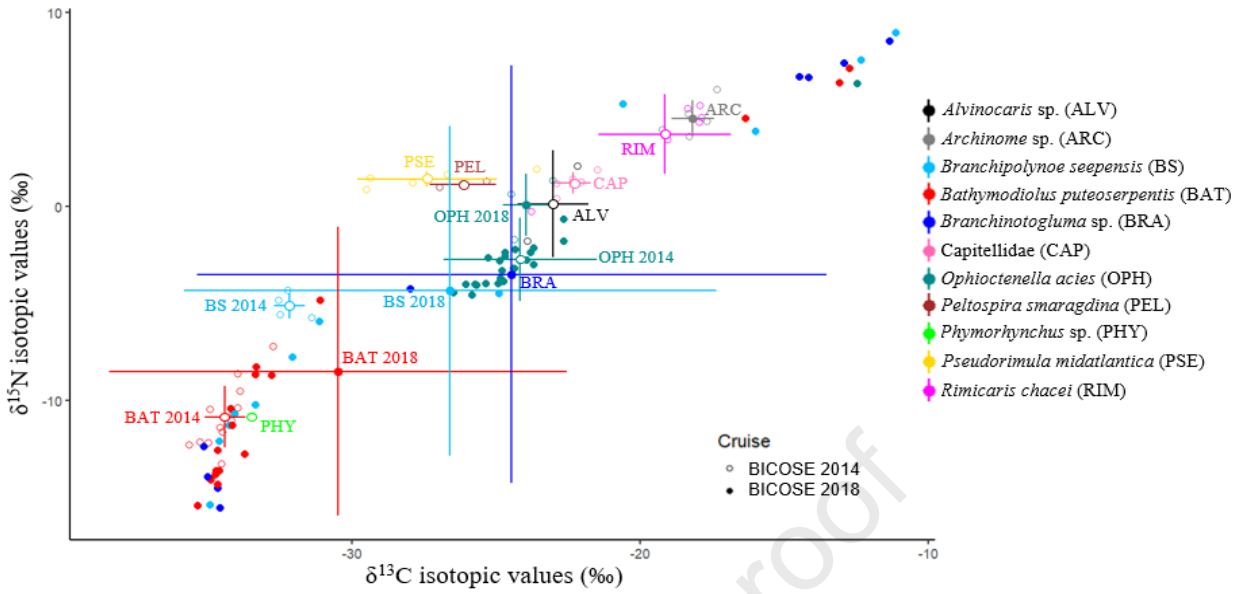

FIGURE 6. Identification of the main groups of organisms sampled on the Moose site from the Snake Pit vent field during the two BICOSE cruises (BICOSE 2014 represented by empty circles, BICOSE 2018 represented by full circles). Groups were identified according to carbon isotopic values (X axis) and nitrogen isotopic values (Y axis). The dots represent the distribution of all the individuals analysed: *Alvinocaris* sp. (n=2); *Archinome* sp. (n=5), *Branchipolynoe seepensis* (n=4 in 2014, n=12 in 2018); *Bathymodiolus puteoserpentis* (n=14 in 2014, n=17 in 2018); *Branchinotogluma* sp. (n=9); Capitellidae (n=5); *Ophioctenella acies* (n=3 in 2014, n=24 in 2018); *Peltospira smaragdina* (n=2); PHY: *Phymorhynchus* sp. (n=1); *Pseudorimula midatlantica* (n=5); *Rimicaris chacei* (n=6).

Hydrothermal shrimps showed high $\delta^{13}C$ values respectively ranging from -23.9‰ to -22.2‰ for *Alvinocaris* sp., and from -23.8 to -17.9‰ for *Rimicaris chacei*, and $\delta^{15}N$ values respectively ranging from -1.8 to 2.1‰ and from -0.3 to 5.2‰, respectively. *Archinome* sp. and *Branchinotogluma* sp. polychaetes showed variable isotopic results: while the former had high values ranging from -19.2‰ to -17.3‰ for $\delta^{13}C$ and from +3.6‰ to +6.0‰ for $\delta^{15}N$, isotopic ratios of the latter were spread across the entire dataset (from -35.2‰ to -11.4‰ for $\delta^{13}C$ and from -15.6‰ to +8.5‰ for $\delta^{15}N$) (Figure 6). Capitellidae polychaetes formed a distinct intermediate group, near *Ophioctenella acies* and *Alvinocaris* sp., with isotopic values ranging from -22.9‰ to -21.5‰ ($\delta^{13}C$) and from +0.4‰ to +1.9‰ ($\delta^{15}N$). Finally, gastropods (including *Pseudorimula midatlantica* and *Peltospira smaragdina*, only sampled in 2014) showed intermediate values from -29.5‰ to -23.6‰ for $\delta^{13}C$ and from +0.9‰ to +1.9‰ for $\delta^{15}N$. The only individual of *Phymorhynchus* sp. gastropod sampled in 2014 had low $\delta^{13}C$ value of -33.5‰ and low $\delta^{15}N$ value of -10.8‰ (Figure 6) close to those of symbiotic species despite its carnivorous nature.

4. Discussion

This study provides a detailed description and characterisation of two *Bathymodiolus puteoserpentis* assemblages colonising the Moose site at the Snake Pit vent field (MAR). Mussel assemblages were suction sampled in triplicate in 2014 at the top of the edifice and in 2018 at its base. The two cruises were carried out with various sampling methods, measuring tools and gear, leading to differences in the physico-chemical

parameters measured. This different sampling effort is due to technical issues and unforeseen events, not allowing an optimal inter-annual comparison. Moreover, the small number of sampling units (n=6) over the two years, makes it difficult to obtain statistically significant results although a clear separation in faunal composition of the two sampling sites (top versus base) was observed. The use of different sampling protocols (sampling in boxes coupled or not with an associated suction sampler) did not seem to influence the results obtained in terms of relative abundance of each taxa, but probably led to an underestimation of faunal abundance and diversity of rarer species on the two sampling units concerned.

4.1. Habitat characterisation

With the exception of SU-1, the temperatures measured above the fauna on the sampling units were relatively uniform, suggesting relatively stable and homogeneous environmental conditions. However, SU-1 exhibited higher temperatures and fluctuations, as shown by a recorded maximum temperature of 15.8°C in the 2014 time series. Located on the top of the edifice, SU-1 also exhibited higher hydrogen sulfide values, suggesting a higher influence of hydrothermal fluids. The average temperatures of the other two SUs at the top were similar to those reported for bottom temperature at this field (i.e. 2.6°C, see Hernández-Ávila et al., 2022). At the edifice base, SU-5 and SU-6 had slightly higher temperatures, as well as lower pH and higher total iron concentrations than SU-4. Their temperatures were closer to those measured at SU-1. These patterns are consistent with the small-scale spatial heterogeneity of physico-chemical conditions characterising the vent environment (Chevaldonné et al., 1991; Johnson et al., 1988; Le Bris et al., 2006; Sarrazin et al., 1999). While they can be used to qualitatively compare the habitats of different assemblages, single-point temperature measurements are not fully representative of the temperatures experienced by the organisms over time. In fact, the deployment of the autonomous temperature probes over time in 2014 showed higher values than those obtained with the submersible sensors for all temperature variables (mean, standard deviation, maximum, minimum) as also reported in a previous study (Marticorena et al., 2021).

In comparison, *Bathymodiolus puteoserpentis* mussels were found at lower temperatures at the Logatchev vent field. Thus, on the Irina II mound, the average temperatures recorded varied between 2.7 ± 0.2°C on a sulfide pillar overgrown by mussels and 3.5 ± 0.7°C on the main assemblage without exceeding 7.4°C (Zielinski et al., 2011). These results corresponded to those obtained for SU-2, SU-3 and SU-4 but not on the other SUs that had higher mean values (up to 9.3°C on SU-1). *B. puteoserpentis* sampled at SP (this study) and Logatchev (Zielinski et al., 2011) were found in habitats colder than those of *Bathymodiolus azoricus*, where the mean temperatures vary between 4.8°C and 10°C (Cuvelier et al., 2011; Desbruyères et al., 2001; Husson et al., 2017).

4.2. Population structure of *Bathymodiolus puteoserpentis*

In the assemblages studied here, *Bathymodiolus puteoserpentis* exhibit large average sizes, with almost all specimens exceeding 5 cm in length. For *Bathymodiolus azoricus*, Cuvelier et al. (2011) identified different types of assemblages, characterised by specific mussel size ranges, with large (≈6 cm), medium (2–6 cm) and small (<2 cm) mussels distributed along a gradient of increasing dilution of the vent fluid (Cuvelier et al., 2009). Since *B. puteoserpentis* and *B. azoricus* exhibit similar body size with maximal shell length of 12 cm in both species (Van Cosel et al. 1999), the same categories could apply to *B. puteoserpentis*. The mussels observed at Snake Pit would therefore correspond to those found in "Assemblage 1" observed by Cuvelier et al. (2011), characterised by larger mussels.

Our results showed that mean mussel shell lengths did not differ significantly between 2014 and 2018. As observed in other MAR mussel assemblages (Cuvelier et al., 2017; Sarradin et al., 1999; Van Audenhaege et al., 2022), the largest mussels were more abundant in the most variable and warmer environment (SU-1) and the smallest in the coldest and least fluctuating environment (SU-2). However, the number of individuals sampled in each SU was too low to statistically support size spatial segregation of mussels, decreasing with increasing distance from hydrothermal input as observed in other studies on *B. azoricus* (Husson et al., 2017; Van Audenhaege et al., 2022). Moreover, our results report the presence of large mussels in colder habitats (SU-3 and SU-4), questioning the presence of a spatial segregation in relation to environmental conditions for *B. puteoserpentis*.

Our video (see Supplementary materials) and *in situ* observations (authors pers. obs.), coupled with our sampling results, denote a general lack of recruitment at the scale of the whole Moose edifice as shown by the predominance of large adult mussels and the near absence of small individuals. The absence of small *B. puteoserpentis* < 5 mm, considered as newly settled juveniles by Van Dover (2002), is consistent with observations by Turnipseed et al. (2004) that reported only 3% of new settlers in July 2001 at the same vent field. This consistent lack of recruitment over the years contrasts with regular observations of new settlers in different *Bathymodiolus* assemblages along the MAR: the presence of small recruits was indeed reported on *B. azoricus* assemblages at the LS vent field (Cuvelier et al. 2009) as well as on *B. puteoserpentis* mussel assemblages on the Semeynov vent field (Franke et al., 2021) and recently close to *Bathymodiolus* sp. on Puy des Folles (MAR, ROV SuBastian's 500th Dive at Puy Des Folles Volcano, 2 April 2023, ~10:15 on the video, https://www.youtube.com/live/C152v5tKl20?si=d-GZAV17MmzxjIPb).

Several abiotic and biotic factors could limit juvenile settlement at vents, in habitats under strong hydrothermal influence and highly fluctuating conditions. Post-larval stages of mussels have no symbionts when they settle at vents and only acquire them progressively afterwards (Wentrup et al., 2013). As symbionts potentially ensure detoxification allowing vent holobionts to better cope with extreme conditions

(Durand et al., 2009, Sun et al. 2022), mussel post-larvae would not be able to handle those prevailing in adult habitat (Husson et al., 2017). However, if larval supply exists, they should be able to settle in peripheral areas with lower hydrothermal influence, which was not observed during our various dives in the area (authors pers. obs.)

Biotic factors could also play a role in settlement. Several studies showed a negative correlation between adults and juveniles in dense coastal mussel assemblages (Khaitov, 2013; Lehane & Davenport, 2004, Okamura, 1986), larval settlement being inhibited by adults. Khaitov and Lentsman (2016) showed that *Mytilus* mussel assemblages in the White Sea follow a cyclical demographic structure, comparable to the ‘‘endogenous’’ model proposed by Lukanin et al. (1986) and which is based on density-dependant regulatory processes. In this model, adult mussels have negative impacts on juvenile conspecifics, both directly via the filtration of larvae, and indirectly via the rejection of pellets “polluting” the environment. This leads to endogenous population instability where only the reduction or disappearance of the adult population would allow the installation of new larvae. In our case, we can hypothesise that *B. puteoserpentis* would be currently at a stage where the population is dominated by old large mussels which inhibit recruitment. Competition with conspecifics and/or other species was also observed on the EPR where juveniles of *Bathymodiolus thermophilus* appear to compete with adult mussels that inhibit their settlement via competition for space and food resources or through intraspecific larviphagy (Comtet and Desbruyères, 1998, Lehane & Davenport, 2004). Finally, mussel juveniles could be also removed by grazers such as Lepetodrilid limpets and other associated species as suggested for other settlers in the vent habitat (Micheli et al., 2002, Lenihan et al., 2008).

The lack of juveniles would result in an aging of the mussel population, and as mortality occurs, to a decrease in the population density of adults. According to the ‘endogenous’ model, two scenarios then seem possible: the cycle can restart with the settlement of new recruits or the colony can die out if the larval supply is not sufficient (Khaitov and Lentsman, 2016). During observations at different time-periods carried out during several French cruises (BICOSE in January 2014, BICOSE2 in February 2018, BICOSE3 in November 2023, HERMINE in March-April 2017, HERMINE2 in July 2022), mussel recruitment patches have not been observed at Snake Pit, even in areas with low mussel densities, which would suggest a lack of larval supply. This may be due to a lack of reproductive individuals locally, and/or a lack of larval input from distant reproductive populations. *B. puteoserpentis* from SP are genetically very close to southern populations at the Logatchev, Puy des Folles and Semeynov vent fields that could have contributed to larval supply (Breusing et al., 2016). However, predominant contemporary migration directions remain to be assessed.

Journal Pre-proof

4.3. Community structure of the associated fauna

Meiofauna largely dominated the overall abundance of the fauna associated with *Bathymodiolus puteoserpentis* on the Moose site, with the exception of SU-1, which exhibited a co-dominance between copepods and *Pseudorimula midatlantica* gastropods. Two SUs were clearly different from the others: SU-5 and SU-6 harboured very high densities of nematodes and copepods, as illustrated by lower equitability evenness and diversity indexes. Copepods colonised habitats with temperatures around 4°C (SU-5/SU-6) and had lower abundance on the slightly colder SU-3 site. This is similar to what was observed by Husson et al. (2017) at the LS vent field where copepods tended to dominate in warmer habitats. Comparing the three 2014 sampling units, the higher densities of nematodes in lower temperature habitats (SU-2/SU-3) were also in accordance with what was observed at LS (Husson et al., 2017), which could explain their low abundance on the warmer and more fluctuating SU-1. In 2018, copepods were no longer dominant at higher temperatures, replaced by nematodes. We can hypothesise that the latter were attracted by higher concentrations of organic matter at the edifice's base, supported by the presence of brittle stars which may be deposit feeders (see below). Overall, meiofaunal densities were lower at the top of the edifice probably linked to harsher environmental conditions and position on the edifice. However, despite our efforts, it was difficult to gather similar physico-chemical parameters on all SUs to discriminate their environmental conditions and specify the niche of each taxa. Finally, a finer taxonomic resolution of the meiofauna would be necessary to refine compositional differences within and between our sampled assemblages.

18 macrofaunal taxa were identified in the 1885 individuals collected in 2014 and 2018. They include 14 different families, with three (Polynoidae, Alvinocarididae and Lepetodrilidae) potentially comprising 2-3 species/morphotypes. This taxonomic richness is only slightly lower than what was obtained by Turnipseed et al. (2004) who identified 22 macrofaunal taxa (excluding *B. puteoserpentis)* from 16 families in a much larger number of individuals sampled (5244 individuals). Nevertheless, anemones and other species of shrimps, such as *Rimicaris exoculata*, although not retrieved in our samples, were observed close to the mussels (See video in the supplementary materials). Macrofaunal densities, ranging from 65 ± 8 to 483.2 ± 69 individuals per litre, were quite similar, and even higher, to those reported by Turnipseed et al. (2004) with 146 ± 120 individuals per litre. Nevertheless, as the volume calculation method differs between the two studies, this comparison may potentially be biassed.

The dominance of *Ophioctenella acies* brittle stars at the base of the studied edifice suggests the presence of a high accumulation of organic matter. The shape of their teeth indicates that they are adapted to sort and grasp the rich source of organic matter produced by the biological activity of mussels and trapped within the assemblage (Tyler et al., 1995). Stöhr and Segonzac (2005) noticed that brittle stars directly positioned

558 themselves on the syphon of mussels evacuating their pseudo-faeces. *O. acies* were previously observed in
559 dense patches (about 20 ind.dm^{-2}) among *B. puteoserpentis* mussels at several hydrothermal fields along the
560 MAR (Tyler et al., 1995). In our study, similar patches have been recorded at the edifice's base (max. of 24
561 ind.dm^{-2} of shell mussels). The activity of mussels holobionts may also impoverish the habitats in sulfides
562 and nitrates while enriching them in ammonia and dissolved organic matter as proposed for *B. azoricus* at
563 two other vent fields of the MAR (LS/MG, Sarradin et al., 2009). These observations support the hypothesis
564 that *O. acies* appear to prefer habitats less directly subjected to hydrothermal fluids, and potentially
565 accumulating higher concentrations of organic matter than the vertical walls of hydrothermal edifices. Thus,
566 we propose that the less turbulent environment at the edifice base (visual observation) would favour the
567 accumulation of organic matter which may be beneficial to brittle stars. This taxa could be considered as an
568 opportunistic species, developing in more turbid and particle-laden habitats, ingesting both organic-rich
569 particles and microbial-coated sulfide particles as proposed by Tyler et al. (1995).

570 *Pseudorimula midatlantica* limpets, dominating the top of the edifice, are known to be the most abundant
571 gastropods on SP and Broken Spur vent fields (Goroslavskaya and Galkin, 2011; Turnipseed et al., 2004).
572 Within *Bathymodiolus azoricus* assemblages at LS, they were found in habitats with higher maximum
573 temperatures than the ophiuroids (10°C versus 6.4°C; Husson et al., 2017). Similar to what we observed in
574 the present study, Turnipseed et al. (2004) listed a spatial segregation between *O. acies* brittle stars and *P.*
575 *midatlantica* limpets on the Moose site. Goroslavskaya and Galkin (2011) also observed a similar pattern.
576 Additional environmental data would be necessary to establish a potential link with species distribution.
577 The quasi-absence of niche overlap between these two macrofaunal dominant species may be linked to
578 competition for resources as they are both detritivorous/bacterivorous. The presence of various
579 microhabitats at vents would allow them to partition their niches according to their respective nutritional
580 needs and physiological tolerances (Lévesque et al. 2006). Beside temperature and sulfide concentrations,
581 other physico-chemical conditions such as substratum and topography could affect vent species distribution
582 (Girard et al., 2020; Sarrazin et al., 1999).

583 Significant differences in faunal abundances, coupled to the macrofaunal composition disparity, between
584 the top and the base of the edifice and between spatially close samples, highlights once again the small-
585 scale heterogeneity of faunal distribution at vents. Differences between sampling units close to each other
586 may be partially explained by unconsidered biotic and abiotic factors including the presence of microbial
587 mats, substratum types or the amount of organic matter for example (Sarrazin et al., 2022). Indeed, the
588 fluctuating environmental conditions, proximity of high temperature emissions and relief may have limited
589 the colonisation by certain taxa at the top of the edifice (lower meiofaunal & macrofaunal densities). In fact,
590 the role of currents and topography on the distribution of vent species has been neglected but recent evidence

591 points for a significant one (Girard et al., 2020; Lelièvre et al., 2017). Our results confirm that the abundance,
592 densities and species richness of the associated fauna were slightly higher in the 2018 samples, consistent
593 with our expectations of having more stable and homogeneous conditions at the base of the edifice, and
594 therefore fewer environmental constraints allowing a higher number of taxa to colonise microhabitats as
595 observed elsewhere at vents (Cuvelier et al., 2009, 2011a; Rybakova Goroslavskaya and Galkin, 2015).
596 Finally, the number of taxa is much higher at LS with a total of 79 taxa compared to 44 taxa at SP, including
597 6 taxa of copepods and 7 taxa of nematodes (Goroslavskaya and Galkin, 2011, Turnipseed et al., 2004,
598 Zekely et al., 2006, this study). Whether this represents the reality or is due, in part, to the much greater
599 sampling effort at LS is unknown. Only with a more extensive and comparable number of samples will we
600 be able to accurately compare the two vent fields.

601 **4.4. Food web**

602 Vent mussels with their autotrophic symbionts are considered as primary producers. Due to chemosynthetic
603 processes converting inorganic carbon into organic compounds, they can be expected to exhibit carbon
604 depletion and hence, a low $\delta^{13}C$ value (Ruby et al., 1987). *Bathymodiolus* spp. at MAR vent fields host both
605 symbiotic thiotrophic and methanotrophic bacteria located in their gills, which provides them with a high
606 plasticity, the proportion of symbionts changing in accordance with the composition of the chemical
607 compounds in their environment (Riou et al., 2008, Duperon et al. 2016). According to the proportion and
608 activity of each type of symbiont, their contribution to the mussel diet varies, and therefore the final $\delta^{13}C$ of
609 the host varies. At LS, thiotrophic bacteria fix inorganic carbon from CO_2, leading to $\delta^{13}C$ values down to -
610 30‰, while methanotrophic bacteria fix methane, leading to carbon isotopic ratios typically down to -20‰
611 (Colaço et al., 2002). In our study, most of the *Bathymodiolus puteoserpentis* mussels were included in the
612 "-30 group" (Colaço et al., 2002) with carbon values very close to -30‰, supporting thiotrophy as the
613 dominant nutritional pathway. These carbon values are in agreement with previous studies carried out on *B.*
614 *puteoserpentis* at the same site (Cavanaugh et al., 1992; Colaço et al., 2002) and on *B. azoricus* sampled on
615 different locations at the LS and MG vent fields, which also displayed average carbon ratios close to -30‰
616 (De Busserolles et al., 2009; Portail et al., 2018).

617 However, isotopic ratios of a few *Bathymodiolus puteoserpentis* individuals collected in 2018 showed more
618 dispersed values, with "marginal" carbon signatures close to -15‰. We hypothesise that this intraspecific
619 variability could indicate a potential fluid resource depletion at the edifice base, inducing the use of a wider
620 range of carbon sources. Portail et al. (2018) assessed the trophic network of *Bathymodiolus azoricus* from
621 northernmost vent fields along the MAR, and identified four potential dominant basal sources:
622 photosynthesis-derived organic matter, autotrophs/thiotrophs using the CBB cycle, autotrophs/thiotrophs

using the rTCA cycle, and methanotrophs. Assuming that carbon sources at the Moose site have similar isotopic signature to those from northern MAR vent fields, isotopic signatures of our "marginal" *B. puteoserpentis* could reflect individuals hosting mainly thiotrophic symbionts using rTCA cycle instead of CBB cycle as in the majority of *Bathymodiolus* mussel. This scenario seems unlikely here as the rTCA cycle is usually favoured in habitats with hypoxic conditions such as those occupied by *Rimicaris exoculata* shrimps (Hügler et al., 2005). Alternatively, they may also indicate the presence of methanotrophic symbionts. However Moose mussels were shown to host low proportions of methanotrophic symbionts (Duperron et al., 2016) reflecting low methane concentrations in their habitat, which is also supported by our data (0.33 µM for SU-1). A third possibility is the reliance on filter feeding, as observed in some *B. azoricus* at LS (De Busserolles et al., 2009; Trask and Van Dover, 1999).

As in previous trophic studies (De Busserolles et al., 2009; Portail et al., 2018), the SP trophic network includes holobionts (*Bathymodiolus puteoserpentis*, *Rimicaris* sp.) as well as detritivores, bacterivores, scavengers and commensal (*Branchipolynoe seepensis*) taxa. However, despite a relatively low species richness, carbon isotope ratios are spread over a wide range of values from -35.6‰ (*B. puteoserpentis*, 2014) to -11.1‰ (*B. seepensis*, 2018) contrary to what was observed on MG and LS vent fields where the $\delta^{13}C$ values were between -20 and -30‰ (Portail et al., 2018). This difference in carbon source distribution between the various vent fields could be explained by several factors such as the physiological diversity among symbiotic and free living microorganisms according to local environmental conditions (Karl, 1995). The association between polynoid scale worms and bathymodiolin mussels are frequent both in the Pacific (Chevaldonné et al., 1998; Lindgren et al., 2019; Pettibone, 1984) and Atlantic (Britaev et al., 2003; Britayev et al., 2003, 2007; Chevaldonné et al., 1998; Cuvelier et al., 2011a; Van Dover et al., 1999; Ward et al., 2004) oceans. In the present study, the isotopic signatures, with a well-differentiated higher trophic level for *Branchipolynoe seepensis* polychaetes, confirm that most of them rely on *B. puteoserpentis*. However, some individuals were occasionally observed outside mussel shells where they normally reside (Sarrazin et al., 2014). The uncommon isotopic ratios of some individuals in the present study could be linked to the three *B. puteoserpentis* specimens having a higher $\delta^{13}C$.

4.5. Climax stage in *B. puteoserpentis* assemblage?

Condition indexes, size structures and biomass values exhibited significant differences between samples, with SU-1 standing out in most cases, reflecting small-scale heterogeneity. Overall, even fewer small and intermediate size mussels were sampled in 2018 at the edifice base compared to the 2014 collection at the top. The dominance of *Ophioctenella acies* in this area suggests a high accumulation of organic matter, potentially due to feces and/or decomposition of dead mussels. This may be confirmed by the identification

of indicative species in the meiofaunal compartment and/or by the measurement of organic matter between sampling sites. The wide carbon isotopic signatures of mussels in 2018 may be due to a lower availability of reduced chemicals at the edifice base. Hypothetically, this situation could have constrained the mussels to seek for other carbon sources, including material sinking from upper oceanic layers. Thus, we hypothesise that *B. puteoserpentis* mussel assemblages could represent a well-established community that has potentially reached a final stage of ecological succession (climax) with few observable recruits at least since 2014. Over time, this may (or not) result in a potential long-term population decline. This hypothesis is supported by the observation of many empty mussel shells at the edifice base during the last French cruises in 2022 and 2023.

5. Conclusion

This study provides additional knowledge on *Bathymodiolus puteoserpentis* assemblages at the Snake Pit vent field (MAR). The two sampling cruises allowed us to show that the species richness of the fauna associated with mussel assemblages appears to be relatively low despite a diversified and extended food web, and a high abundance of certain taxa. The local edifice-scale heterogeneity of the fauna was partially explained by variations in environmental conditions such as temperatures, fluid proximity and the location of the assemblage on the edifice. Other non-measured physico-chemical factors such as the availability of food sources, substratum types, topography and currents remain to be evaluated. Regarding the engineer species *B. puteoserpentis*, very little recruitment was observed in 2014 and 2018 at the edifice and vent field scales. The widening of the food web and uncommon isotopic signatures of some *B. puteoserpentis* individuals potentially show a search for food diversification. These observations suggest that chemosynthetic pathways may not be carried out at least in some places of the site. Large mussels were still observed 5 years after this study during the BICOSE 3 cruise (2023), which opened the way for an alternative hypothesis: *B. puteoserpentis* population could have reached and still be in a climax state. This raises questions about the future of this community in the years to come. In fact, various scenarios can be considered, ranging from the potential decline of the community which appears to chronically lack renewal through recruitment, to the complete renewal of the population by a settlement event triggered by the release of larvae at a time when the community feels threatened. A complementary study will have to be carried out to validate or not this hypothesis, while continuing the physico-chemical and taxonomic characterization of these mussel assemblages and their associated fauna.

Data availability statement

The datasets and video images presented in this study can be found in online repositories. Metadata from the various cruises are provided here: CAMBON-BONAVITA Marie-Anne (2014) BICOSE cruise, RV *Pourquoi pas?*, https://doi.org/10.17600/14000100; CAMBON-BONAVITA Marie-Anne (2018) BICOSE 2 cruise, RV Pourquoi pas?, https://doi.org/10.17600/18000004.

Credit author statement

Alicia Veuillot: formal analysis, visualisation, writing – original draft, **Florence Pradillon:** conceptualization, methodology, supervision, writing – review & editing, **Loïc N. Michel:** resources, writing – review & editing, **Cécile Cathalot:** formal analysis, resources, writing – review & editing, **Marie-Anne Cambon:** funding acquisition, methodology, supervision, writing – review & editing, **Jozée Sarrazin:** conceptualization, funding acquisition, methodology, supervision, writing – review & editing.

Funding

The thesis of the first author has been granted by a fellowship from the Region Bretagne - ARED 2021 and co-supported by the Ifremer REMIMA Project. The project also benefited from BiodivRestore ERA-NET Cofund (GA N°101003777).

Acknowledgments

We thank the captain of the R/Vs *Pourquoi pas ?* and their crews for their collaboration in the success of the cruises. We are grateful to Marie-Anne Cambon, chief scientist who supported our sampling program. We are also grateful to the Nautile and ROV Victor6000 pilots for their patience and constant support. We warmly thank the LEP technical team for its valuable help both at sea and in the lab. Five undergraduate students contributed to sorting the fauna, carrying out isotopic and biomass analyses: Erwann Legrand (MsC 2 2014), Anne-Mathilde Brochard (MSc 1 2015), Bruno Labelle (MSc 2, 2015), Liz Loutrage (MSc 1, 2018), Flavie Vasnier (L2, 2022). This research is part of the DEEP REST project that was funded through the 2020-2021 Biodiversa and Water JPI joint call for research projects, under the BiodivRestore ERA-NET Cofund (GA N°101003777), with the EU and the following funding organisations: Agence Nationale de la Recherche (ANR-21-BIRE-0003), France, Ministry of Agriculture, Nature and Food Quality (LNV), Netherlands, Research Foundation – Flanders (FWO), Belgium, German Federal Ministry of Research (BMBF) through VDI/VDE-IT, Germany, Environmental Protection Agency (EPA), Ireland, Fundação para a Ciência e a Tecnologia (FCT), Portugal, Fundo Regional para a Ciência e Tecnologia (FRCT), Portugal-Azores and State Research Agency (AEI), Spain. This work is also granted by ARED-Région Bretagne 2021 and Ifremer REMIMA Project.

Journal Pre-proof

Supplementary materials

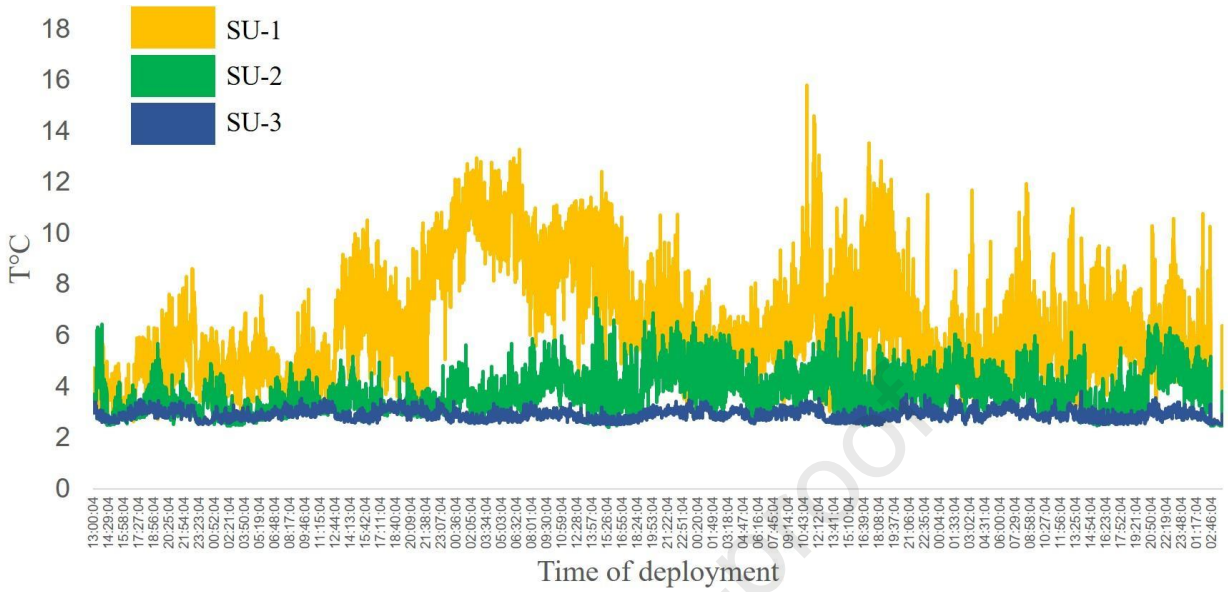

Supplementary Figure S1. Temperature variations in sampling units SU-1, SU-2 and SU-3 from the top of the Moose edifice at the Snake Pit vent field (Mid-Atlantic Ridge). Temperatures were taken just above the mussels every 30 seconds during 4 days and 14 hours with MISO autonomous probes.

Supplementary video. Video of the Moose edifice where we can notice the absence of small mussels on the entire sulfide edifice. https://video.ifremer.fr/video?id=12092

References

Bergquist, D., Eckner, J., Urcuyo, I., Cordes, E., Hourdez, S., Macko, S., Fisher, C., 2007. Using stable isotopes and quantitative community characteristics to determine a local hydrothermal vent food web. Mar. Ecol. Prog. Ser. 330, 49–65. https://doi.org/10.3354/meps330049

Breusing, C., Biastoch, A., Drews, A., Metaxas, A., Jollivet, D., Vrijenhoek, R.C., Bayer, T., Melzner, F., Sayavedra, L., Petersen, J.M., Dubilier, N., Schilhabel, M.B., Rosenstiel, P., Reusch, T.B.H., 2016. Biophysical and Population Genetic Models Predict the Presence of "Phantom" Stepping Stones Connecting Mid-Atlantic Ridge Vent Ecosystems. Curr. Biol. 26, 2257–2267. https://doi.org/10.1016/j.cub.2016.06.062

Bris, N.L., Rodier, P., Sarradin, P.-M., Gall, C.L., 2006. Is temperature a good proxy for sulfide in hydrothermal vent habitats ? Cah. Biol. Mar 47, 465-470

Britaev, T.A., Krylova, E.M., Aksyuk, T.S., Cosel, R., 2003. Association of Atlantic Hydrothermal Mytilids of the Genus *Bathymodiolus spp*. (Mollusca: Mytilidae) with the Polychaeta B*ranchipolynoe aff. seepensis* (Polychaeta: Polynoidae): Commensalism or Parasitism? Dokl. Biol. Sci. 391, 371-374.

Britayev, T.A., Krylova, E.M., Martin, D., von Cosel, R., Aksiuk, T.S., Martín D., 2003. Symbiont – host interaction in the association of the scale worm *Branchipolynoe* aff. *seepensis* (Polychaeta: Polynoidae) with the hydrothermal mussel *Bathymodiolus*spp. (Bivalvia: Mytilidae). *InterRidge News*, 12(2), 13-16.

738 Britayev, T.A., Martin, D., Krylova, E.M., von Cosel, R., Aksiuk, T.S., 2007. Life-history traits of the symbiotic
739 scale-worm Branchipolynoe seepensis and its relationships with host mussels of the genus Bathymodiolus
740 from hydrothermal vents. Mar. Ecol. 28, 36–48. https://doi.org/10.1111/j.1439-0485.2007.00152.x

741 Brown, J.R., Karson, J.A., 1988. Variations in axial processes on the Mid-Atlantic Ridge: The median valley
742 of the MARK area. Mar. Geophys. Res. 10, 109–138. https://doi.org/10.1007/BF02424663

743 Campbell, B.J., Cary, S.C., 2004. Abundance of Reverse Tricarboxylic Acid Cycle Genes in Free-Living
744 Microorganisms at Deep-Sea Hydrothermal Vents. AEM 70 (10).
745 https://doi.org/10.1128/AEM.70.10.6282-6289.2004

746 Cavanaugh, C.M., Wirsen, C.O., Jannasch, H.W., 1992. Evidence for Methylotrophic Symbionts in a
747 Hydrothermal Vent Mussel (Bivalvia: Mytilidae) from the Mid-Atlantic Ridge. Appl. Environ. Microbiol. 58,
748 3799–3803. https://doi.org/10.1128/aem.58.12.3799-3803.1992

749 Charlou, J.L., Donval, J.P., Douville, E., Jean-Baptiste, P., Radford-Knoery, J., Fouquet, Y., Dapoigny, A.,
750 Stievenard, M., 2000. Compared geochemical signatures and the evolution of Menez Gwen (37°50'N) and
751 Lucky Strike (37°17'N) hydrothermal fluids, south of the Azores Triple Junction on the Mid-Atlantic Ridge.
752 Chem. Geol. 171, 49-75.

753 Charlou, J.L., Donval, J.P., Fouquet, Y., Jean-Baptiste, P., Holm, N., 2002. Geochemistry of high H2 and CH4
754 vent fluids issued from ultramafic rocks at the Rainbow hydrothermal field (36°14'N, MAR). Chem. Geol.
755 191, 345-359.

756 Charlou, J.L., Donval, J.P., Konn, C., Ondréas, H., Fouquet, Y., Jean-Baptiste, P., Fourré, E., 2010. High
757 production and fluxes of H2 and CH4 and evidence of abiotic hydrocarbon synthesis by serpentinization in
758 ultramafic-hosted hydrothermal systems on the Mid-Atlantic Ridge, in: Rona, P.A., Devey, C.W., Dyment,
759 J., Murton, B.J. (Eds.), Geophysical Monograph Series. American Geophysical Union, Washington, D. C., pp.
760 265–296. https://doi.org/10.1029/2008GM000752

761 Chevaldonné, P., Desbruyères, D., Haître, M.L., 1991. Time-series of temperature from three deep-sea
762 hydrothermal vent sites. Deep Sea Res. Part Oceanogr. Res. Pap. 38, 1417–1430.
763 https://doi.org/10.1016/0198-0149(91)90014-7

764 Chevaldonné, P., Jollivet, D., Feldman, R.A., Desbruyères, D., Lutz, R.A., Vrijenhoek, R.C., 1998. Commensal
765 scale-worms of the genus Branchipolynoe (Polychaeta: Polynoidae) at deep-sea hydrothermal vents and
766 cold seeps. Cah. Biol. Mar. 39, 347-350.

767 Colaço, A., Dehairs, F., Desbruyères, D., 2002. Nutritional relations of deep-sea hydrothermal fields at the
768 Mid-Atlantic Ridge: a stable isotope approach. Deep Sea Res. Part Oceanogr. Res. Pap. 49, 395–412.
769 https://doi.org/10.1016/S0967-0637(01)00060-7

770 Colaço, A., Martins, I., Laranjo, M., Pires, L., Leal, C., Prieto, C., Costa, V., Lopes, H., Rosa, D., Dando, P.R.,
771 Serrão-Santos, R., 2006. Annual spawning of the hydrothermal vent mussel, *Bathymodiolus azoricus*, under
772 controlled aquarium conditions at atmospheric pressure. J. Exp. Mar. Biol. Ecol. 333, 166 – 171.

773 Comtet, T., Desbruyères, D., 1998. Population structure and recruitment in mytilid bivalves from the Lucky
774 Strike and Menez Gwen hydrothermal vent fields (37°17'N and 37°50'N on the Mid-Atlantic Ridge). Mar.
775 Ecol. Prog. Ser. 163, 165–177. https://doi.org/10.3354/meps163165

Journal Pre-proof

776 Coplen, T.B., 2011. Guidelines and recommended terms for expression of stable-isotope-ratio and gas-
777 ratio measurement results. Rapid Commun. Mass Spectrom. 25, 2538–2560.
778 https://doi.org/10.1002/rcm.5129

779 Cucherousset, J., Villéger, S., 2015. Quantifying the multiple facets of isotopic diversity: New metrics for
780 stable isotope ecology. Ecol. Indic. 56, 152–160. https://doi.org/10.1016/j.ecolind.2015.03.032

781 Cuvelier, D., Legendre, P., Laës-Huon, A., Sarradin, P.-M., Sarrazin, J., 2017. Biological and environmental
782 rhythms in (dark) deep-sea hydrothermal ecosystems. Biogeosciences 14, 2955–2977.
783 https://doi.org/10.5194/bg-14-2955-2017

784 Cuvelier, D., Sarradin, P.-M., Sarrazin, J., Colaço, A., Copley, J.T., Desbruyères, D., Glover, A.G., Santos, R.S.,
785 Tyler, P.A., 2011a. Hydrothermal faunal assemblages and habitat characterisation at the Eiffel Tower
786 edifice (Lucky Strike, Mid-Atlantic Ridge): Hydrothermal faunal assemblages and habitat characterisation
787 of the Eiffel Tower. Mar. Ecol. 32, 243–255. https://doi.org/10.1111/j.1439-0485.2010.00431.x

788 Cuvelier, D., Sarrazin, J., Colaço, A., Copley, J., Desbruyères, D., Glover, A.G., Tyler, P., Serrão Santos, R.,
789 2009. Distribution and spatial variation of hydrothermal faunal assemblages at Lucky Strike (Mid-Atlantic
790 Ridge) revealed by high-resolution video image analysis. Deep Sea Res. Part Oceanogr. Res. Pap. 56, 2026–
791 2040. https://doi.org/10.1016/j.dsr.2009.06.006

792 Cuvelier, D., Sarrazin, J., Colaço, A., Copley, J.T., Glover, A.G., Tyler, P.A., Santos, R.S., Desbruyères, D.,
793 2011. Community dynamics over 14 years at the Eiffel Tower hydrothermal edifice on the Mid-Atlantic
794 Ridge. Limnol. Oceanogr. 56, 1624–1640. https://doi.org/10.4319/lo.2011.56.5.1624

795 De Busserolles, F., Sarrazin, J., Gauthier, O., Gélinas, Y., Fabri, M.C., Sarradin, P.M., Desbruyères, D., 2009.
796 Are spatial variations in the diets of hydrothermal fauna linked to local environmental conditions? Deep
797 Sea Res. Part II Top. Stud. Oceanogr. 56, 1649–1664. https://doi.org/10.1016/j.dsr2.2009.05.011

798 DeNiro, M.J., Epstein, S., 1978. Influence of diet on the distribution of carbon isotopes in animals. Geochim.
799 Cosmochim. Acta 42, 495–506. https://doi.org/10.1016/0016-7037(78)90199-0

800 Desbruyères, D., Biscoito, M., Caprais, J.-C., Colaço, A., Comtet, T., Crassous, P., Fouquet, Y., Khripounoff,
801 A., Le Bris, N., Olu, K., Riso, R., Sarradin, P.-M., Segonzac, M., Vangriesheim, A., 2001. Variations in deep-
802 sea hydrothermal vent communities on the Mid-Atlantic Ridge near the Azores plateau. Deep Sea Res. Part
803 Oceanogr. Res. Pap. 48, 1325–1346. https://doi.org/10.1016/S0967-0637(00)00083-2

804 Distel, D.L., Lee, H.K., Cavanaugh, C.M., 1995. Intracellular Coexistence of Methano- and Thioautotrophic
805 Bacteria in a Hydrothermal Vent Mussel. Proc. Natl. Acad. Sci. 92, 9598–9602.
806 https://doi.org/10.1073/pnas.92.21.9598

807 Duperron, S., Bergin, C., Zielinski, F., Blazejak, A., Pernthaler, A., McKiness, Z.P., DeChaine, E., Cavanaugh,
808 C.M., Dubilier, N., 2006. A dual symbiosis shared by two mussel species, *Bathymodiolus azoricus* and
809 *Bathymodiolus puteoserpentis* (Bivalvia: Mytilidae), from hydrothermal vents along the northern Mid-
810 Atlantic Ridge. Environ. Microbiol. 8, 1441–1447. https://doi.org/10.1111/j.1462-2920.2006.01038.x

811 Duperron, S., Quiles, A., Szafranski, K.M., Léger, N., Shillito, B., 2016. Estimating Symbiont Abundances and
812 Gill Surface Areas in Specimens of the Hydrothermal Vent Mussel *Bathymodiolus puteoserpentis*
813 Maintained in Pressure Vessels. Front. Mar. Sci. 3. https://doi.org/10.3389/fmars.2016.00016

Journal Pre-proof

Durand, L., Zbinden, M., Cueff-Gauchard, V., Duperron, S., Roussel, E.G., Shillito, B., Cambon-Bonavita, M.A., 2009. Microbial diversity associated with the hydrothermal shrimp *Rimicaris exoculata* gut and occurrence of a resident microbial community. FEMS Microb. Ecol. 71, 291-303. https://doi.org/10.1111/j.1574-6941.2009.00806.x

Durant, C., Ballu, V., Gente, P., Dubois, J., 1996. Horst and graben structures on the flanks of the Mid-Atlantic ridge in the MARK area (23°22'N): Submersible observations. Tectonophysics 265, 275–297. https://doi.org/10.1016/S0040-1951(96)00049-2

Fisher, C.R., Brooks, J.M., Vodenichar, J.S., Zande, J.M., Childress, J.J., Jr., R.A.B., 1993. The Co-occurrence of Methanotrophic and Chemoautotrophic Sulfur-Oxidizing Bacterial Symbionts in a Deep-sea Mussel. Mar. Ecol. 14, 277–289. https://doi.org/10.1111/j.1439-0485.1993.tb00001.x

Fisher, C.R., Childress, J.J., Arp, A.J., Brooks, J.M., Distel, D., Favuzzi, J.A., Felbeck, H., Hessler, R., Johnson, K.S., Kennicutt, M.C., Macko, S.A., Newton, A., Powell, M.A., Somero, G.N., Soto, T., 1988. Microhabitat variation in the hydrothermal vent mussel, B*athymodiolus thermophilus*, at the Rose Garden vent on the Galapagos Rift. Deep Sea Res. Part Oceanogr. Res. Pap. 35, 1769–1791. https://doi.org/10.1016/0198-0149(88)90049-0

Fouquet, Y., Cambon, P., Etoubleau, J., Charlou, J.L., Ondréas, H., Barriga, F.J.A.S., Cherkashov, G., Semkova, T., Poroshina, I., Bohn, M., Donval, J.P., Henry, K., Murphy, P., Rouxel, O., 2010. Geodiversity of Hydrothermal Processes Along the Mid-Atlantic Ridge and Ultramafic-Hosted Mineralization: A New Type of Oceanic Cu-Zn-Co-Au Volcanogenic Massive Sulfide Deposit. Geophys. Monogr. Ser. 188 https://doi.org/10.1029/2008GM000746

Franke, M., Geier, B., Hammel, J.U., Dubilier, N., Leisch, N., 2021. Coming together—symbiont acquisition and early development in deep-sea bathymodiolin mussels. Proc. R. Soc. B. 288, 20211044. https://doi.org/10.1098/rspb.2021.1044

Galkin, S.V., Goroslavskaya, E.I., 2010. Bottom fauna associated with *Bathymodiolus azoricus* (Mytilidae) mussel beds in the hydrothermal fields of the Mid-Atlantic Ridge. Oceanology 50, 51–60. https://doi.org/10.1134/S0001437010010066

Gebruk, A.V., Southward, E.C., Kennedy, H., Southward, A.J., 2000. Food sources, behaviour, and distribution of hydrothermal vent shrimps at the Mid-Atlantic Ridge. J. Mar. Biol. Assoc. U. K. 80, 485–499. https://doi.org/10.1017/S0025315400002186

Girard, F., Sarrazin, J., Arnaubec, A., Cannat, M., Sarradin, P.-M., Wheeler, B., Matabos, M., 2020. Currents and topography drive assemblage distribution on an active hydrothermal edifice. Prog. Oceanogr. 187, 102397. https://doi.org/10.1016/j.pocean.2020.102397

Gollner, S., Colaço, A., Gebruk, A., Halpin, P.N., Higgs, N., Menini, E., Mestre, N.C., Qian, P.-Y., Sarrazin, J., Szafranski, K., Van Dover, C.L., 2021. Application of scientific criteria for identifying hydrothermal ecosystems in need of protection. Mar. Policy 132, 104641. https://doi.org/10.1016/j.marpol.2021.104641

Gollner, S., Govenar, B., Fisher, C., Bright, M., 2015. Size matters at deep-sea hydrothermal vents: different diversity and habitat fidelity patterns of meio- and macrofauna. Mar. Ecol. Prog. Ser. 520, 57–66. https://doi.org/10.3354/meps11078

Goroslavskaya, E.I., Galkin, S.V., 2011. Benthic fauna associated with mussel beds and shrimp swarms at hydrothermal fields on the Mid-Atlantic Ridge. Oceanology 51, 69–79. https://doi.org/10.1134/S0001437011010048

Govenar, B., 2010. Shaping Vent and Seep Communities: Habitat Provision and Modification by Foundation Species. The Vent and Seep Biota, TGBI. 33, 403–432. https://doi.org/10.1007/978-90-481-9572-5_13

Govenar, B., Fisher, C.R., 2007. Experimental evidence of habitat provision by aggregations of *Riftia pachyptila* at hydrothermal vents on the East Pacific Rise. Mar. Ecol. 28, 3–14. https://doi.org/10.1111/j.1439-0485.2007.00148.x

Govenar, B., Le Bris, N., Gollner, S., Glanville, J., Aperghis, A., Hourdez, S., Fisher, C., 2005. Epifaunal community structure associated with *Riftia pachyptila* aggregations in chemically different hydrothermal vent habitats. Mar. Ecol. Prog. Ser. 305, 67–77. https://doi.org/10.3354/meps305067

Henry, M.S., Childress, J.J., Figueroa, D., 2008. Metabolic rates and thermal tolerances of chemoautotrophic symbioses from Lau Basin hydrothermal vents and their implications for species distributions. Deep Sea Res. Part Oceanogr. Res. Pap. 55, 679–695. https://doi.org/10.1016/j.dsr.2008.02.001

Hernández-Ávila, I., Cambon-Bonavita, M.-A., Sarrazin, J., Pradillon, F., 2022. Population structure and reproduction of the alvinocaridid shrimp *Rimicaris exoculata* on the Mid-Atlantic Ridge: Variations between habitats and vent fields. Deep Sea Res. Part Oceanogr. Res. Pap. 186, 103827. https://doi.org/10.1016/j.dsr.2022.103827

Hunt, H.L., Metaxas, A., Jennings, R.M., Halanych, K.M., Mullineaux, L.S., 2004. Testing biological control of colonization by vestimentiferan tubeworms at deep-sea hydrothermal vents (East Pacific Rise, 9°50'N). Deep Sea Res. Part Oceanogr. Res. Pap. 51, 225–234. https://doi.org/10.1016/j.dsr.2003.10.008

Husson, B., Sarradin, P.-M., Zeppilli, D., Sarrazin, J., 2017. Picturing thermal niches and biomass of hydrothermal vent species. Deep Sea Res. Part II Top. Stud. Oceanogr. 137, 6–25. https://doi.org/10.1016/j.dsr2.2016.05.028

Jackson, A.L., Inger, R., Parnell, A.C., Bearhop, S., 2011. Comparing isotopic niche widths among and within communities: SIBER - Stable Isotope Bayesian Ellipses in R: Bayesian isotopic niche metrics. J. Anim. Ecol. 80, 595–602. https://doi.org/10.1111/j.1365-2656.2011.01806.x

Johnson, K.S., Childress, J.J., Beehler, C.L., 1988. Short-term temperature variability in the Rose Garden hydrothermal vent field: an unstable deep-sea environment. Deep Sea Res. Part Oceanogr. Res. Pap. 35, 1711–1721. https://doi.org/10.1016/0198-0149(88)90045-3

Karl, D.M., 1995. Ecology of free-living, hydrothermal vent microbial communities. *Microbiol*. Deep-Sea Hydrothermal Vents.

Karson, J.A., Thompson, G., Humphris, S.E., Edmond, J.M., Bryan, W.B., Brown, J.R., Winters, A.T., Pockalny, R.A., Casey, J.F., Campbell, A.C., Klinkhammer, G., Palmer, M.R., Kinzler, R.J., Sulanowska, M.M., 1987. Along-axis variations in seafloor spreading in the MARK area. Nature 328, 681–685. https://doi.org/10.1038/328681a0

Khaitov, V.M., 2013. Life in an unstable house: community dynamics in changing mussel beds. Hydrobiologia 706, 139-158.

Khaitov, V.M., Lentsman, N.V., 2016. The cycle of mussels: long-term dynamics of mussel beds on intertidal soft bottoms at the White Sea. Hydrobiologia 781, 161–180. https://doi.org/10.1007/s10750-016-2837-0

Lalou, C., Reyss, J., Brichet, E., Arnold, M., Thompson, G., Fouquet, Y., Rona, P.A., 1993. New age data for Mid-Atlantic Ridge hydrothermal sites: TAG and Snakepit chronology revisited. J. Geophys. Res. Solid Earth 98, 9705–9713. https://doi.org/10.1029/92JB01898

Layman, C.A., Arrington, D.A., Montaña, C.G., Post, D.M., 2007. Can stable isotope ratios provide for community-wide measures of trophic structure? Ecology 88, 42–48. https://doi.org/10.1890/0012-9658(2007)88[42:CSIRPF]2.0.CO;2

Lehane, C., Davenport, J., 2004. Ingestion of bivalve larvae by *Mytilus edulis*: experimental and field demonstrations of larviphagy in farmed blue mussels. Mar. Biol. 145, 101-107.

Lelièvre, Y., Legendre, P., Matabos, M., Mihály, S., Lee, R.W., Sarradin, P.-M., Arango, C.P., Sarrazin, J., 2017. Astronomical and atmospheric impacts on deep-sea hydrothermal vent invertebrates. Proc. R. Soc. B Biol. Sci. 284, 20162123. https://doi.org/10.1098/rspb.2016.2123

Lelièvre, Y., Sarrazin, J., Marticorena, J., Schaal, G., Day, T., Legendre, P., Hourdez, S., Matabos, M., 2018. Biodiversity and trophic ecology of hydrothermal vent fauna associated with tubeworm assemblages on the Juan de Fuca Ridge. Biogeosciences 15, 2629–2647. https://doi.org/10.5194/bg-15-2629-2018

Lenihan, H.S., 1999. Physical-biological coupling on oyster reefs : how habitat structure influences individual performance. Ecol. Monogr. 69, 251–275. https://doi.org/10.1890/0012-9615(1999)069[0251:PBCOOR]2.0.CO;2

Lenihan, H.S., Mills, S.W., Mullineaux, L.S., Peterson, C.H., Fisher, C.R., Micheli, F., 2008. Biotic interactions at hydrothermal vents: Recruitment inhibition by the mussel *Bathymodiolus thermophilus*. Deep Sea Res. Part Oceanogr. Res. Pap. 55, 1707–1717. https://doi.org/10.1016/j.dsr.2008.07.007

Levesque, C., Juniper, S., Marcus, J., 2003. Food resource partitioning and competition among alvinellid polychaetes of Juan de Fuca Ridge hydrothermal vents. Mar. Ecol. Prog. Ser. 246, 173–182. https://doi.org/10.3354/meps246173

Levesque, C., Kim Juniper, S., Limén, H., 2006. Spatial organization of food webs along habitat gradients at deep-sea hydrothermal vents on Axial Volcano, Northeast Pacific. Deep Sea Res. Part Oceanogr. Res. Pap. 53, 726–739. https://doi.org/10.1016/j.dsr.2006.01.007

Levin, L.A., Michener, R.H., 2002. Isotopic evidence for chemosynthesis-based nutrition of macrobenthos: The lightness of being at Pacific methane seeps. Limnol. Oceanogr. 47, 1336–1345. https://doi.org/10.4319/lo.2002.47.5.1336

Lindgren, J., Hatch, A.S., Hourdez, S., Seid, C.A., Rouse, G.W., 2019. Phylogeny and Biogeography of Branchipolynoe (Polynoidae, Phyllodocida, Aciculata, Annelida), with Descriptions of Five New Species from Methane Seeps and Hydrothermal Vents. Diversity 11, 153. https://doi.org/10.3390/d11090153

Journal Pre-proof

Lukanin, V.V., Naumov A.D., Fedyakov V.V., 1986. The cyclic development of Mytilus edulis L. populations in the White Sea. Doklady Akademii Nauk SSSR 287: 78–84. (in Russian).

Luther, G.W., Rozan, T.F., Taillefert, M., Nuzzio, D.B., Di Meo, C., Shank, T.M., Lutz, R.A., Cary, S.C., 2001. Chemical speciation drives hydrothermal vent ecology. Nature 410, 813–816. https://doi.org/10.1038/35071069

Lutz, R.A., Kennish, M.J., 1993. Ecology of deep-sea hydrothermal vent communities: A review. Rev. Geophys. 31, 211. https://doi.org/10.1029/93RG01280

Maas, P.A.Y., O'Mullan, G.D., Lutz, R.A., Vrijenhoek, R.C., 1999. Genetic and Morphometric Characterization of Mussels (Bivalvia: Mytilidae) From Mid-Atlantic Hydrothermal Vents. Biol. Bull. 196, 265–272. https://doi.org/10.2307/1542951

Marticorena, J., Matabos, M., Ramirez-Llodra, E., Cathalot, C., Laes-Huon, A., Leroux, R., Hourdez, S., Donval, J.-P., Sarrazin, J., 2021. Recovery of hydrothermal vent communities in response to an induced disturbance at the Lucky Strike vent field (Mid-Atlantic Ridge). Mar. Environ. Res. 168, 105316. https://doi.org/10.1016/j.marenvres.2021.105316

Martins, I., Colaço, A. , Dando, P.R., Martins, I. , Desbruyères, D., Sarradin P.M., Marques J.C., Serrao-Santos, R., 2008. Size-dependent variations on the nutritional pathway of *Bathymodiolus azoricus* demonstrated by a C-flux model. Ecol Modell. 217, 59-71. https://doi.org/10.1016/j.ecolmodel.2008.05.008

Matabos, M., Cuvelier, D., Brouard, J., Shillito, B., Ravaux, J., Zbinden, M., Barthelemy, D., Sarradin, P.M., Sarrazin, J., 2015. Behavioural study of two hydrothermal crustacean decapods: *Mirocaris fortunata* and *Segonzacia mesatlantica,* from the Lucky Strike vent field (Mid-Atlantic Ridge). Deep Sea Res. Part II Top. Stud. Oceanogr. 121, 146–158. https://doi.org/10.1016/j.dsr2.2015.04.008

Mateo, M.A., Serrano, O., Serrano, L., Michener, R.H., 2008. Effects of sample preparation on stable isotope ratios of carbon and nitrogen in marine invertebrates: implications for food web studies using stable isotopes. Oecologia 157, 105–115. https://doi.org/10.1007/s00442-008-1052-8

McCutchan, J.H., Lewis, W.M., Kendall, C., McGrath, C.C., 2003. Variation in trophic shift for stable isotope ratios of carbon, nitrogen, and sulfur. OIKOS 102, 378–390. https://doi.org/10.1034/j.1600-0706.2003.12098.x

Methou, P., Hernández-Ávila, I., Cathalot, C., Cambon-Bonavita, M., Pradillon, F., 2022. Population structure and environmental niches of Rimicaris shrimps from the Mid-Atlantic Ridge. Mar. Ecol. Prog. Ser. 684, 1–20. https://doi.org/10.3354/meps13986

Micheli, F., Peterson, C.H., Mullineaux, L.S., Fisher, C.R., Mills, S.W., Sancho, G., Johnson, G.A., Lenihan, H.S., 2002. Predation Structures Communities at Deep-Sea Hydrothermal Vents. Ecol. Monogr. 72, 365–382. https://doi.org/10.1890/0012-9615(2002)072[0365:PSCADS]2.0.CO;2

Molodtsova, T.N., Galkin, S.V., Kobyliansky, S.G., Simakova, U.V., Vedenin, A.A., Dobretsova, I.G., Gebruk, A.V., 2017. First data on benthic and fish communities from the Mid-Atlantic Ridge, 16°40′– 17°14′N. Deep Sea Res. Part II Top. Stud. Oceanogr. 137, 69–77. https://doi.org/10.1016/j.dsr2.2016.10.006

Journal Pre-proof

Moore, T.S., Shank, T.M., Nuzzio, D.B., Luther, G.W., 2009. Time-series chemical and temperature habitat characterization of diffuse flow hydrothermal sites at 9°50'N East Pacific Rise. Deep Sea Res. Part II Top. Stud. Oceanogr. 56, 1616–1621. https://doi.org/10.1016/j.dsr2.2009.05.008

Mullineaux, L.S., Fisher, C.R., Peterson, C.H., Schaeffer, S.W., 2000. Tubeworm succession at hydrothermal vents: use of biogenic cues to reduce habitat selection error? Oecologia 123, 275–284. https://doi.org/10.1007/s004420051014

Mullineaux, L.S., Peterson, C.H., Micheli, F., Mills, S.W., 2003. Successional mechanism varies along a gradient in hydrothermal fluid flux at deep-sea vents. Ecol. Monogr. 73, 523–542. https://doi.org/10.1890/02-0674

Nedoncelle, K., Lartaud, F., Contreira Pereira, L., Yücel, M., Thurnherr, A.M., Mullineaux, L., Le Bris, N., 2015. Bathymodiolus growth dynamics in relation to environmental fluctuations in vent habitats. Deep Sea Res. Part Oceanogr. Res. Pap. 106, 183–193. https://doi.org/10.1016/j.dsr.2015.10.003

Nedoncelle, K., Lartaud, F., de Rafelis, M., Boulila, S., Le Bris, N., 2013. A new method for high-resolution bivalve growth rate studies in hydrothermal environments. Mar. Biol. 160, 1427–1439. https://doi.org/10.1007/s00227-013-2195-7

Okamura, B., 1986. Group living and the effects of spatial position in aggregations of *Mytilus edulis*. Oecologia 69, 341-347.

O'Mullan, G.D., Maas, P. a. Y., Lutz, R.A., Vrijenhoek, R.C., 2001. A hybrid zone between hydrothermal vent mussels (Bivalvia: Mytilidae) from the Mid-Atlantic Ridge. Mol. Ecol. 10, 2819–2831. https://doi.org/10.1046/j.0962-1083.2001.01401.x

Page, H.M., Fiala-Medioni, A., Fisher, C.R., Childress, J.J., 1991. Experimental evidence for filter-feeding by the hydrothermal vent mussel, *Bathymodiolus thermophilus*. Deep Sea Res. Part Oceanogr. Res. Pap. 38, 1455–1461. https://doi.org/10.1016/0198-0149(91)90084-S

Pettibone, M.H., 1986. A new scale-worm commensal with deep-sea mussels in the seep-sites at the Florida Escarpment in the Eastern Gulf of Mexico. (Polychaeta: Polynoidae: Branchipolynoinae). Proc. Biol. Soc. Wash. 99(3), 444-451.

Pettibone, M.H., 1984. A new scale-worm commensal with deep-sea mussels on the Galapagos hydrothermal vent (Polychaeta: Polynoidae). Proc. Biol. Soc. Wash 97(1), 226-239.

Piquet, B., Le Panse, S., Lallier, F.H., Duperron, S., Andersen, A.C., 2022. "There and back again" - Ultrastructural changes in the gills of Bathymodiolus vent-mussels during symbiont loss: Back to a regular filter-feeding epidermis. Front. Mar. Sci. 9, 968331. https://doi.org/10.3389/fmars.2022.968331

Podowski, E., Ma, S., Luther, G., Wardrop, D., Fisher, C., 2010. Biotic and abiotic factors affecting distributions of megafauna in diffuse flow on andesite and basalt along the Eastern Lau Spreading Center, Tonga. Mar. Ecol. Prog. Ser. 418, 25–45. https://doi.org/10.3354/meps08797

Portail, M., Brandily, C., Cathalot, C., Colaço, A., Gélinas, Y., Husson, B., Sarradin, P.-M., Sarrazin, J., 2018. Food-web complexity across hydrothermal vents on the Azores triple junction. Deep Sea Res. Part Oceanogr. Res. Pap. 131, 101–120. https://doi.org/10.1016/j.dsr.2017.11.010

Journal Pre-proof

Portail, M., Olu, K., Dubois, S.F., Escobar-Briones, E., Gelinas, Y., Menot, L., Sarrazin, J., 2016. Food-Web Complexity in Guaymas Basin Hydrothermal Vents and Cold Seeps. PLoS ONE 11, e0162263. https://doi.org/10.1371/journal.pone.0162263

Raulfs, E.C., Macko, S.A., Van Dover, C.L., 2004. Tissue and symbiont condition of mussels (*Bathymodiolus thermophilus*) exposed to varying levels of hydrothermal activity. J. Mar. Biol. Ass. UK 84, 229–234. https://doi.org/10.1017/S0025315404009087h

Rigolet, C., Thiébaut, E., Brind'Amour, A., Dubois, S.F., 2015. Investigating isotopic functional indices to reveal changes in the structure and functioning of benthic communities. Funct. Ecol. 29, 1350–1360. https://doi.org/10.1111/1365-2435.12444

Riou, V., Halary, S., Duperron, S., Bouillon, S., Elskens, M., Bettencourt, R., Santos, R.S., Dehairs, F., Colaço, A., 2008. Influence of CH_4 and H_2S availability on symbiont distribution, carbon assimilation and transfer in the dual symbiotic vent mussel *Bathymodiolus azoricus*. Biogeosciences 5, 1681-1691. https://doi.org/10.5194/bg-5-1681-2008

Ruby, E.G., Jannasch, H.W., Deuser, W.G., 1987. Fractionation of Stable Carbon Isotopes during Chemoautotrophic Growth of Sulfur-Oxidizing Bacteria. Appl. Environ. Microbiol. 53, 1940–1943. https://doi.org/10.1128/aem.53.8.1940-1943.1987

Rybakova Goroslavskaya, E., Galkin, S., 2015. Hydrothermal assemblages associated with different foundation species on the East Pacific Rise and Mid-Atlantic Ridge, with a special focus on mytilids. Mar. Ecol. 36, 45–61. https://doi.org/10.1111/maec.12262

Sarradin, P.-M., Caprais, J.-C., Riso, R., Kerouel, R., Aminot, A., 1999. Chemical environment of the hydrothermal mussel communities in the Lucky Strike and Menez Gwen vent fields, Mid Atlantic Ridge. Cah. Biol. Mar. 40, 93-104.

Sarradin, P.-M., Waeles, M., Bernagout, S., Le Gall, C., Sarrazin, J., Riso, R., 2009. Speciation of dissolved copper within an active hydrothermal edifice on the Lucky Strike vent field (MAR, 37°N). Sci. Total Environ. 407, 869–878. https://doi.org/10.1016/j.scitotenv.2008.09.056

Sarrazin, J., Cathalot, C., Laes, A., Marticorena, J., Michel, L.N., Matabos, M., 2022. Integrated Study of New Faunal Assemblages Dominated by Gastropods at Three Vent Fields Along the Mid-Atlantic Ridge: Diversity, Structure, Composition and Trophic Interactions. Front. Mar. Sci. 9, 925419. https://doi.org/10.3389/fmars.2022.925419

Sarrazin, J., Cuvelier, D., Peton, L., Legendre, P., Sarradin, P.M., 2014. High-resolution dynamics of a deep-sea hydrothermal mussel assemblage monitored by the EMSO-Açores MoMAR observatory. Deep Sea Res. Part Oceanogr. Res. Pap. 90, 62–75. https://doi.org/10.1016/j.dsr.2014.04.004

Sarrazin, J., Juniper, S., Massoth, G., Legendre, P., 1999. Physical and chemical factors influencing species distributions on hydrothermal sulfide edifices of the Juan de Fuca Ridge, northeast Pacific. Mar. Ecol. Prog. Ser. 190, 89–112. https://doi.org/10.3354/meps190089

Sarrazin, J., Legendre, P., de Busserolles, F., Fabri, M.-C., Guilini, K., Ivanenko, V.N., Morineaux, M., Vanreusel, A., Sarradin, P.-M., 2015. Biodiversity patterns, environmental drivers and indicator species on

a high-temperature hydrothermal edifice, Mid-Atlantic Ridge. Deep Sea Res. Part II Top. Stud. Oceanogr. 121, 177–192. https://doi.org/10.1016/j.dsr2.2015.04.013

Sarrazin, J., Portail, M., Legrand, E., Cathalot, C., Laes, A., Lahaye, N., Sarradin, P.M., Husson, B., 2020. Endogenous versus exogenous factors: What matters for vent mussel communities? Deep Sea Res. Part Oceanogr. Res. Pap. 160, 103260. https://doi.org/10.1016/j.dsr.2020.103260

Sarrazin, J., Robigou, V., Juniper, S., Delaney, J., 1997. Biological and geological dynamics over four years on a high-temperature sulfide structure at the Juan de Fuca Ridge hydrothermal observatory. Mar. Ecol. Prog. Ser. 153, 5–24. https://doi.org/10.3354/meps153005

Sen, A., Podowski, E.L., Becker, E.L., Shearer, E.A., Gartman, A., Yücel, M., Hourdez, S., Luther, G.W.I., Fisher, C.R., 2014. Community succession in hydrothermal vent habitats of the Eastern Lau Spreading Center and Valu Fa Ridge, Tonga. Limnol. Oceanogr. 59, 1510–1528. https://doi.org/10.4319/lo.2014.59.5.1510

Sievert, S.M., Brinkhoff, T., Muyzer, G., Ziebis, W., Kuever, J., 1999. Spatial Heterogeneity of Bacterial Populations along an Environmental Gradient at a Shallow Submarine Hydrothermal Vent near Milos Island (Greece). Appl. Environ. Microbiol. 65, 3834–3842. https://doi.org/10.1128/AEM.65.9.3834-3842.1999

Stöhr, S., Segonzac, M., 2005. Deep-sea ophiuroids (Echinodermata) from reducing and non-reducing environments in the North Atlantic Ocean. J. Mar. Biol. Assoc. U. K. 85, 383–402. https://doi.org/10.1017/S0025315405011318h

Sun, Y., Wang, M., Zhong, Z., Chen, H., Wang, H., Zhou, L., Cao, L., Fu, L., Zhang, H., Lian, C., Sun, S., Li, C., 2022. Adaption to hydrogen sulfide-rich environments: Strategies for active detoxification in deep-sea symbiotic mussels, *Gigantidas platifrons*. Sci. Total Environ. 804, 150054. https://doi.org/10.1016/j.scitotenv.2021.150054

Trask, J.L., Van Dover, C.L., 1999. Site-specific and ontogenetic variations in nutrition of mussels (*Bathymodiolus* sp.) from the Lucky Strike hydrothermal vent field, Mid-Atlantic Ridge. Limnol. Oceanogr. 44, 334–343. https://doi.org/10.4319/lo.1999.44.2.0334

Tunnicliffe, V., 1991. The Biology of Hydrothermal Vents - Ecology and Evolution. Oceanogr. Mar. Biol. 29, 319–407.

Turnipseed, M., Jenkins, C.D., Van Dover, C.L., 2004. Community structure in Florida Escarpment seep and Snake Pit (Mid-Atlantic Ridge) vent mussel beds. Mar. Biol. 145, 121–132. https://doi.org/10.1007/s00227-004-1304-z

Turnipseed, M., Knick, K.E., Lipcius, R.N., Dreyer, J., Van Dover, C.L., 2003. Diversity in mussel beds at deep-sea hydrothermal vents and cold seeps. Ecol. Lett. 6, 518–523. https://doi.org/10.1046/j.1461-0248.2003.00465.x

Tyler, P.A., Paterson, G.J.L., Sibuet, M., f-Guille, A., Murton, B.J., Segonzac, M., 1995. A New Genus of Ophiuroid (Echinodermata: Ophiuroidea) from Hydrothermal Mounds Along The Mid-Atlantic Ridge. J. Mar. Biol. Assoc. U. K. 75, 977–986. https://doi.org/10.1017/S0025315400038303

Journal Pre-proof

1073 Van Audenhaege, L., Matabos, M., Brind'Amour, A., Drugmand, J., Laës-Huon, A., Sarradin, P.-M., Sarrazin,
1074 J., 2022. Long-term monitoring reveals unprecedented stability of a vent mussel assemblage on the Mid-
1075 Atlantic Ridge. Prog. Oceanogr. 204, 102791. https://doi.org/10.1016/j.pocean.2022.102791

1076 Van Cosel R., Comtet, T., Krylova, E.M., 1999. Bathymodiolus (Bivalvia: mytilidae) from hydrothermal vents
1077 on the Azores triple junction and the Logatchev hydrothermal field. Atl. Ridge. Veliger 42, 218-248.

1078 Van Dover, C., 2003. Variation in community structure within hydrothermal vent mussel beds of the East
1079 Pacific Rise. Mar. Ecol. Prog. Ser. 253, 55–66. https://doi.org/10.3354/meps253055

1080 Van Dover, C., 2002. Community structure of mussel beds at deep-sea hydrothermal vents. Mar. Ecol.
1081 Prog. Ser. 230, 137–158. https://doi.org/10.3354/meps230137

1082 Van Dover, C., Trask, J., Gross, J., Knowlton, A., 1999. Reproductive biology of free-living and commensal
1083 polynoid polychaetes at the Lucky Strike hydrothermal vent field (Mid-Atlantic Ridge). Mar. Ecol. Prog. Ser.
1084 181, 201–214. https://doi.org/10.3354/meps181201

1085 Vismann, B., 2012. Sulfide tolerance: Physiological mechanisms and ecological implications. Ophelia.

1086 Vuillemin, R., Le Roux, D., Dorval, P., Bucas, K., Sudreau, J.P., Hamon, M., Le Gall, C., Sarradin, P.M., 2009.
1087 CHEMINI: A new in situ CHEmical MINIaturized analyzer. Deep Sea Res. Part Oceanogr. Res. Pap. 56, 1391–
1088 1399. https://doi.org/10.1016/j.dsr.2009.02.002

1089 Ward, M., Shields, J., Van Dover, C., 2004. Parasitism in species of Bathymodiolus (Bivalvia: Mytilidae)
1090 mussels from deep-sea seep and hydrothermal vents. Dis. Aquat. Organ. 62, 1–16.
1091 https://doi.org/10.3354/dao062001

1092 Wentrup, C., Wendeberg, A., Huang, J.Y., Borowski, C., Dubilier, N., 2013. Shift from widespread symbiont
1093 infection of host tissues to specific colonization of gills in juvenile deep-sea mussels. The ISME Journal 7,
1094 1244-1247. https://doi.org/10.1038/ismej.2013.5

1095 Zekely, J., Van Dover, C.L., Nemeschkal, H.L., Bright, M., 2006. Hydrothermal vent meiobenthos associated
1096 with mytilid mussel aggregations from the Mid-Atlantic Ridge and the East Pacific Rise. Deep Sea Res. Part
1097 Oceanogr. Res. Pap. 53, 1363–1378. https://doi.org/10.1016/j.dsr.2006.05.010

1098 Zielinski, F.U., Gennerich, H.-H., Borowski, C., Wenzhöfer, F., Dubilier, N., 2011. In situ measurements of
1099 hydrogen sulfide, oxygen, and temperature in diffuse fluids of an ultramafic-hosted hydrothermal vent
1100 field (Logatchev, 14°45'N, Mid-Atlantic Ridge): Implications for chemosymbiotic bathymodiolin mussels.
1101 Geochem. Geophys. Geosystems 12(9). https://doi.org/10.1029/2011GC003632

1102 Zilber-Rosenberg, I., Rosenberg, E., 2008. Role of microorganisms in the evolution of animals and plants:
1103 the hologenome theory of evolution. FEMS Microbiol. Rev. 32, 723–735. https://doi.org/10.1111/j.1574-
1104 6976.2008.00123.

Journal Pre-proof

Journal Pre-proof

Highlights

- Assemblage heterogeneity at different scales linked to fluid proximity & location.
- Meiofaunal groups dominated. Macrofaunal disparity between top and base of edifice.
- Low number of mussel juveniles over time questions the future of the population.

Journal Pre-proof

Journal Pre-proof

Declaration of interests

☒ The authors declare that they have no known competing financial interests or personal relationships that could have appeared to influence the work reported in this paper.

☐ The authors declare the following financial interests/personal relationships which may be considered as potential competing interests:

Journal Pre-proof